ESAIM: M2AN 60 (2026) 25–50
https://doi.org/10.1051/m2an/2025094

ESAIM: Mathematical Modelling and Numerical Analysis
www.esaim-m2an.org

RESIDUAL-BASED *A POSTERIORI* ERROR ESTIMATION FOR A SPACE-TIME DISCONTINUOUS GALERKIN FORMULATION OF THE RICHARDS EQUATION

Scott Congreve[1,*] and Hyun-Geun Shin[2]

Abstract. In this article, we develop the *a posteriori* error analysis of a space-time discontinuous Galerkin finite element method for the Richards equation. Computable upper and lower bounds on the error in a residual dual norm are derived, which are explicit in the mesh size. Several numerical experiments demonstrate the performance of the *a posteriori* error bound within an mesh refinement algorithm, which refines the mesh as time evolves. Although this *a posteriori* error bound is on the residual dual norm, and is not a upper bound for the H^1-norm, it is able to refine the areas of the mesh where the residual is large in a manner which reduces the H^1-error and L^2-error as well.

Mathematics Subject Classification. 65N15, 65N30, 65N50.

Received January 27, 2025. Accepted November 25, 2025.

1. Introduction

In this article, we develop an *a posteriori* error analysis for the space-time discontinuous Galerkin method (STDG) for the Richards equation. The Richards equation [42] models fluid flows in variably saturated porous media, and is utilized in many areas such as agriculture and hydrology. The pressure formulation is given as

$$\partial_t \vartheta(u) - \nabla \cdot (\mathbf{K}(u)\nabla u) = f \qquad \text{in } \Omega \times (0,T), \tag{1}$$

$$u = 0 \qquad \text{on } \partial\Omega \times (0,T), \tag{2}$$

$$u(\cdot,0) = u_0 \qquad \text{in } \Omega. \tag{3}$$

Here, $\Omega \subset \mathbb{R}^2$ is a bounded polygonal domain with boundary $\partial\Omega$, $T > 0$, ∂_t is the derivative with respect to time, $u : \Omega \times (0,T) \to \mathbb{R}$ is the normalized pressure function with initial condition $u_0 : \Omega \to \mathbb{R}$, $f : \Omega \times (0,T) \to \mathbb{R}$ is the source term, $\mathbf{K} : \mathbb{R} \to \mathbb{R}^{2\times 2}$ is the hydraulic conductivity tensor, $\theta : \mathbb{R} \to \mathbb{R}$ is the water content function, and $\vartheta : \mathbb{R} \to \mathbb{R}$ is the active pore volume defined by

$$\vartheta(u) = \theta(u) + \frac{S_s}{\theta_s} \int_{-\infty}^{u} \theta(s)\,\mathrm{d}s, \tag{4}$$

Keywords and phrases. Richards' equation, *a posteriori* error estimates, space-time discontinuous Galerkin, adaptive refinement.

[1] Faculty of Mathematics and Physics, Charles University, Sokolovská 83, 186 75 Praha, Czech Republic.
[2] Department of Mathematical Sciences, University of Texas at El Paso, El Paso, TX 79968, USA.
*Corresponding author: congreve@karlin.mff.cuni.cz

where $S_s, \theta_s \geq 0$ are material parameters. We assume that the water content ϑ is non-negative, non-decreasing, and Lipschitz continuous and that the hydraulic conductivity $\mathbf{K}$ is symmetric, positively semi-definite, and Lipschitz continuous. The Richards equation can be considered as a nonlinear degenerative parabolic equation [18] as it can degenerate to either an elliptic equation (*fast-diffusion* degeneracy) or to a system of ordinary differential equations (*slow-diffusion degeneracy*). The concept of fast and slow diffusions was described in [37] by mentioning the experimental results on the curves of different models of hydraulic conductivity and water content. We note that this is only one possible formulation of a Richards equation in broad sense depending on if it is pressure-based (as in this case), saturation-based, or mixed, and whether the hydraulic head is normalized; cf. for example, [21, 43, 44] for a comparison between different formulations.

The existence and uniqueness of a weak solution in $\mathrm{L}^2([0,T],\mathrm{H}^1(\Omega))$ for the Richards equation was first shown in [3], with Dirichlet and Neumann boundary conditions. Moreover, existence of viscosity solutions are sought in [34]. Furthermore, the existence of strong solutions are studied under the condition of constant pressure gradient in [12].

Due to the nonlinearity and possibility of degeneracy the efficient computation of a numerical solution to the Richards equation is challenging; cf. [32]. Several numerical methods have been proposed and analyzed, such as conforming finite element methods [24, 39], finite volume methods [30, 31], mixed finite elements [7, 41, 49, 50], and a mixed finite volume-finite element [40]. Additionally, several variants of discontinuous Galerkin finite element methods have been studied [11, 16, 26, 36].

The Richards equation (1) was solved in [21] with the interior penalty (IP) [8, 20] variant of the space-time discontinuous Galerkin finite element method. In particular, it was demonstrated that the STDG with temporal and spatial adaptations exhibits an efficient simulation of practical problems in porous media flow. The discontinuous nature of the method allows approximation of discontinuous and more stable sharp gradients in the solution, such as boundary layers. However, only a practical implementation is provided, and no error estimation was performed. *A priori* error estimation for a semi-discrete spatial discretization *via* a *local discontinuous Galerkin* formulation has been studied in [17]. In this article, we will study a residual-type *a posteriori* error estimation of the IP STDG method, and its use in driving the spatial adaptation.

Upper bounds for residual-type *a posteriori* error estimates on quasilinear parabolic partial differential equations for finite volume [25] and finite element [9, 27, 47] spatial discretization for the method of lines have been analyzed in the case where the time derivative is linear; hence, the challenge is only in the nonlinear diffusion term. Upper and lower bounds have been derived for a p-Laplacian operator which is assumed to be strictly monotone [15]. In [22] an equilibrated flux reconstruction technique [14, 19, 28] for the *a posteriori* error estimate for nonlinear diffusion with both continuous and discontinuous Galerkin space-time formulations has been studied. Degenerate nonlinear parabolic problems with linear time derivative has been studied with low order spatial and temporal discretization methods such as the $P1$-finite element [35] and finite volume [1] with backward Euler.

Based on those results analysis for the Richards equation has been studied in various articles. In [10] only the upper bounds for a formulation using multistep and finite volume method was derived for a version of the Richards equation with nonlinear water content function and a bounded conductivity. A discontinuous Galerkin formulation with a backwards difference formula in time was studied in [16] without derivation of lower bounds, [38] studied a finite element method for a hydraulic conductivity bounded by positive constants, and [13] studied a mixed finite element with implicit Euler. For a space-time discontinuous Galerkin formulation of the Richards equation [23] adopted the technique from [22] to derive *a posteriori* error estimators based on a equilibrated flux reconstruction. This technique requires additional local computations in order to compute the error bounds. Furthermore, the scaling parameter and the defined norm in the analysis can be complicated.

In this article, we instead conduct a residual-based *a posteriori* error analysis, cf. [48], to derive the upper and lower bounds for the numerical approximation of the Richards equation (1)–(3) by the space-time discontinuous Galerkin formulation. Here, as well as deriving both upper and lower bounds, which is often missing in the above analysis, we also can compute the error estimate without any additional formulations or computations. Specifically, we demonstrate how to estimate both the time and space jump terms.

The article is organized as follows. In Section 2 we state the space-time discontinuous Galerkin formulation of (1)–(3). The upper and lower *a posteriori* error bounds are derived in Section 3. Section 4 contains a set of numerical experiments to validate the performance of adaptive refinement based on the *a posteriori* error indicators. Finally, in Section 5 we summarise the main results of this article.

2. Space-time discontinuous Galerkin formulation

In this section, we discretize the Richards equation (1)–(3) using the *incomplete interior penalty* (IIP) *space-time discontinuous Galerkin* finite element method; cf. [21]. To this end, we first introduce the necessary notation.

2.1. Meshes, spaces, and trace operators

We consider the partition of the time interval $(0,T)$ into s sub-intervals $I_m = (t_{m-1}, t_m)$, $m = 1, \dots, s$, with time step $\tau_m = t_m - t_{m-1}$. For $m = 1, \dots, s$, we consider shape-regular meshes $\mathcal{T}_h^m$ that partition the domain Ω into disjoint triangles K such that $\overline{\Omega} = \bigcup_{K \in \mathcal{T}_h^m} \overline{K}$. We assume each mesh is conforming; *i.e.*, the mesh does not contain hanging nodes. We denote by h_K the element diameter for each element $K \in \mathcal{T}_h^m$. On a mesh $\mathcal{T}_h^m$ we can define the broken H^k-space, for $k \geq 1$ as

$$\mathrm{H}^k(\Omega, \mathcal{T}_h^m) = \big\{\phi \in \mathrm{L}^2(\Omega) : \phi|_K \in \mathrm{H}^k(K), K \in \mathcal{T}_h^m\big\},$$

with associated norm

$$\|v\|^2_{\mathrm{H}^k(\Omega,\mathcal{T}_h^m)} \coloneqq \sum_{K \in \mathcal{T}_h^m} \|v\|^2_{\mathrm{H}^k(K)}.$$

Let $p \geq 0$ be an integer and $P_p(K)$ be the space of polynomial functions of total degree p on an element $K \in \mathcal{T}_h^m$, $m = 1, \dots, s$; then, we can define the finite element space

$$S_{h,p}^m = \big\{\phi \in \mathrm{L}^2(\Omega) : \phi|_K \in P_p(K), K \in \mathcal{T}_h^m\big\}.$$

Furthermore, for an integer $q \geq 0$ let $P_q(I_m, S_{h,p}^m)$ be the space of the tensor product of a polynomial function in time of degree q with the space $S_{h,p}^m$ such that for a function $\phi \in P_q(I_m, S_{h,p}^m)$ it holds that $\phi(\cdot, t) \in S_{h,p}^m$ for all $t \in I_m$. Then, we define the space-time finite element space

$$S_{h,p}^{\tau,q} = \big\{\phi \in \mathrm{L}^2(I_m, \mathrm{L}^2(\Omega)) : \phi|_{I_m} \in P_q\big(I_m, S_{h,p}^m\big), m = 1, \dots, s\big\}.$$

We now define some suitable edge operators required for the definition of the STDG. To this end, we denote by $\mathcal{F}_{h,I}^m$ and $\mathcal{F}_{h,D}^m$ the set of interior and boundary faces, respectively, of the mesh $\mathcal{T}_h^m$, $m = 1, \dots, s$, and let $\mathcal{F}_h^m = \mathcal{F}_{h,I}^m \cup \mathcal{F}_{h,D}^m$. For an edge $\gamma \in \mathcal{F}_h^m$ we denote by h_γ the length of the edge. Let v and $\mathbf{q}$ be scalar- and vector-valued functions, respectively, which are smooth inside each element $K \in \mathcal{T}_h^m$. Given two adjacent elements $K^+, K^- \in \mathcal{T}_h^m$ which share a common edge $\gamma \in \mathcal{F}_{h,I}^m$ we write $v^\pm$ and $\mathbf{q}^\pm$ to denote the traces of v and $\mathbf{q}$ from the interior of $K^\pm$, respectively, and define $\mathbf{n}_\gamma$ as the outward unit normal to K^+ on the edge. We now define the average of v and $\mathbf{q}$ at $\mathbf{x} \in \gamma$ as

$$\{\!\{v\}\!\} = \frac{1}{2}\big(v^+ + v^-\big) \qquad \{\!\{\mathbf{q}\}\!\} = \frac{1}{2}\big(\mathbf{q}^+ + \mathbf{q}^-\big)$$

and the jumps of v and $\mathbf{q}$ at $\mathbf{x} \in \gamma$ as

$$[\![v]\!] = \big(v^+ - v^-\big) \qquad [\![\mathbf{q}]\!] = \big(\mathbf{q}^+ - \mathbf{q}^-\big).$$

On a boundary face $\gamma \in \mathcal{F}_{h,D}^m$, we set $\{\!\{v\}\!\} = v$, $\{\!\{\mathbf{q}\}\!\} = \mathbf{q}$, $[\![v]\!] = v$, and $[\![\mathbf{q}]\!] = \mathbf{q}$.

For $v \in S_{h,p}^{\tau,q}$ we let

$$v_m^- = \lim_{t \to t_m^-} v(t), \quad m = 1, \dots, s, \qquad v_m^+ = \lim_{t \to t_m^+} v(t), \quad m = 0, \dots, s-1,$$

and define the time jump

$$\lfloor v \rfloor_m = v_m^+ - v_m^-, \quad m = 1, \dots, s-1, \qquad \lfloor v \rfloor_0 = v_m^+ - u_0.$$

2.2. Incomplete interior penalty STDG discretization

In this section, we define the incomplete interior penalty STDG for the numerical approximation of (1)–(3), cf. [21]. Given a time partition $\{I_m\}_{m=1}^s$, with corresponding meshes $\{\mathcal{T}_h^m\}_{m=1}^s$, and time and space polynomial degrees p and q, respectively, we seek a numerical approximation $u_h^\tau \in S_{h,p}^{\tau,q}$ such that

$$A_{h,m}(u_h^\tau, v_h^\tau) = \ell(v_h^\tau), \tag{5}$$

for all $v_h^\tau \in S_{h,p}^{\tau,q}$, $m = 1, \dots, s$, where

$$A_{h,m}(u,v) = \int_{I_m} (\partial_t \vartheta(u), v)_{\mathcal{T}_h^m} + a_{h,m}(u,v)\,\mathrm{d}t + (\lfloor \vartheta(u) \rfloor_{m-1}, v_{m-1}^+)_{\mathcal{T}_h^m}, \tag{6}$$

$$a_{h,m}(u,v) = (\mathbf{K}(u)\nabla u, \nabla v)_{\mathcal{T}_h^m} - \sum_{\gamma \in \mathcal{F}_h^m} (\mathbf{n}_\gamma \cdot \{\!\{\mathbf{K}(u)\nabla u\}\!\}, [\![v]\!])_\gamma + \sum_{\gamma \in \mathcal{F}_h^m} \epsilon([\![u]\!], [\![v]\!])_\gamma, \tag{7}$$

$$\ell(v) = \int_{I_m} (f, v)_{\mathcal{T}_h^m}\,\mathrm{d}t, \tag{8}$$

for $m = 1, \dots, s$. Here, $(\cdot,\cdot)_{\mathcal{T}_h^m} = \sum_K (\cdot,\cdot)_K$, and $(\cdot,\cdot)_K$ and $(\cdot,\cdot)_\gamma$ denote the L^2-inner product for an element $K \in \mathcal{T}_h^m$ and edge $\gamma \in \mathcal{F}_h^m$, respectively. The parameter ϵ is given by

$$\epsilon = \frac{C_W}{h_\gamma}$$

where $C_W > 0$ is the penalization constant.

Remark 2.1. In the case of an inhomogeneous boundary condition $u = g$ on $\partial\Omega$ the linear functional $\ell(v)$ is replaced by

$$\ell(v) = \int_{I_m} (f, v)_{\mathcal{T}_h^m} + \sum_{\gamma \in \mathcal{F}_{h,D}^m} \epsilon (g, v)_\gamma;$$

cf. [21].

3. *A posteriori* ERROR ANALYSIS

In this section, we follow the technique presented in Section 3.8 of [48] to derive a residual-based error estimate for (5). We first define the dual norm

$$\|\!|\mathcal{R}(u)|\!\|_m = \sup_{v \in \mathrm{L}^2(I_m, \mathrm{H}^1(\Omega, \mathcal{T}_h^m)) \setminus \{0\}} \frac{\langle \mathcal{R}(u), v \rangle}{\|v\|_{\mathrm{L}^2(I_m, \mathrm{H}^1(\Omega, \mathcal{T}_h^m))}}, \tag{9}$$

for $u \in \mathrm{L}^2(I_m, \mathrm{H}^1(\Omega, \mathcal{T}_h^m))$, where

$$\langle \mathcal{R}(u), v \rangle := \ell(v) - A_{h,m}(u,v). \tag{10}$$

Remark 3.1. We note that this dual norm is defined on the broken space $\mathrm{H}^1(\Omega, \mathcal{T}_h^m)$ as it is the dual for the broken H^1-norm and needs to apply on the broken finite element space. We note that this is similar to how the residual is defined in other discontinuous space-time methods; cf. for example equation (19) of [22] which uses the $L^2(I_m, L^2(\Omega))$-space.

For $v \in \mathrm{L}^2(I_m, \mathrm{H}^1(\Omega, \mathcal{T}_h^m))$ and $u_h^\tau \in S_{h,p}^{\tau,q}$, we have

$$\langle \mathcal{R}(u_h^\tau), v \rangle = \ell(v) - A_{h,m}(u_h^\tau, v) = A_{h,m}(u,v) - A_{h,m}(u_h^\tau, v). \tag{11}$$

3.1. Auxiliary results

Before deriving the *a posteriori* error estimates we define the following auxiliary results. To this end, we first define the set of vertices of the mesh $\mathcal{T}_h^m$ as $\mathcal{N}_h$, the set of vertices for each element $K \in \mathcal{T}_h^m$ as $\mathcal{N}_K$, and the set of vertices of each edge $\gamma \in \mathcal{F}_h^m$ as $\mathcal{N}_\gamma$. At each vertex $\mathbf{z} \in \mathcal{N}_h$ we define the hat function λ_z, and let ω_z denote the patch of elements sharing the vertex $\mathbf{z}$.

Lemma 3.2. *Let λ_z be the hat function at vertex $\mathbf{z}$. For $w \in \mathrm{H}^1(K)$ and $w_h \in P_0(K)$, $\lambda_z(w - w_h)$ on an element $K \in \omega_z$ is zero on at least one edge γ. Then,*

$$\left\|\lambda_z^{1/2}(w - w_h)\right\|_{\mathrm{L}^2(K)} \leq C_F(K) h_K \left\|\lambda_z^{1/2}\nabla w\right\|_{\mathrm{L}^2(K)},$$

where

$$C_F(K) = \sup_{w \in \mathrm{H}^1(K)\setminus\{0\}} \frac{\|\lambda_z^{1/2}(w - w_h)\|_{\mathrm{L}^2(K)}}{h_K \|\lambda_z^{1/2}\nabla w\|_{\mathrm{L}^2(K)}}.$$

Proof. See [48], p. 105. □

Lemma 3.3. *Let $w \in \mathrm{H}^1(\Omega, \mathcal{T}_h^m)$, then we can estimate the average term $\{\!\{\cdot\}\!\}$ and the jump term $[\![\cdot]\!]$ as*

$$\sum_{\gamma \in \mathcal{F}_h^m} \int_\gamma \{\!\{w\}\!\}^2 \,\mathrm{d}s \leq \sum_{K \in \mathcal{T}_h^m} \int_{\partial K} |w|^2 \,\mathrm{d}s \tag{12}$$

$$\sum_{\gamma \in \mathcal{F}_h^m} \int_\gamma [\![w]\!]^2 \,\mathrm{d}s \leq 2 \sum_{K \in \mathcal{T}_h^m} \int_{\partial K} |w|^2 \,\mathrm{d}s. \tag{13}$$

Proof. See Lemma 2.27 of [20] for the second result. The first result follows similarly. □

Lemma 3.4. *Let $w \in \mathrm{H}^1(K)$, $K \in \mathcal{T}_h^m$; then, for $\gamma \in \partial K$*

$$\left\|\lambda_z^{1/2} w\right\|_{\mathrm{L}^2(\gamma)}^2 \leq \frac{3\mu_1(\gamma)}{2\mu_2(K)} \left\|\lambda_z^{1/2} w\right\|_{\mathrm{L}^2(K)}^2 + \frac{h_K \mu_1(\gamma)}{\mu_2(K)} \left\|\lambda_z^{1/2} w\right\|_{\mathrm{L}^2(K)} \left\|\lambda_z^{1/2}\nabla w\right\|_{\mathrm{L}^2(K)}$$

where $\mu_1(\gamma)$ and $\mu_2(K)$ is the Lebesgue measure of γ and K, respectively.

Proof. We first define $\mathbf{r}_{K,\gamma}(\mathbf{x}) = \mathbf{x} - \mathbf{a}_{K,\gamma}$, where $\mathbf{a}_{K,\gamma}$ is the vertex of the element K opposite the edge γ; then, by Proposition 3.2 of [48] for $\lambda_z v \in \mathrm{W}^{1,1}(K)$

$$\frac{1}{\mu_1(\gamma)} \int_\gamma \lambda_z v \,\mathrm{d}s - \frac{1}{\mu_2(K)} \int_K \lambda_z v \,\mathrm{d}\mathbf{x} = \frac{1}{2\mu_2(K)} \int_K \mathbf{r}_{K,\gamma} \cdot \nabla(\lambda_z v) \,\mathrm{d}\mathbf{x}.$$

From Proposition 3.3 of [48], using $\mathbf{r}_{K,\gamma} \cdot \nabla\lambda_z = \lambda_z$

$$\frac{1}{\mu_1(\gamma)} \int_\gamma \lambda_z v \,\mathrm{d}s - \frac{3}{2\mu_2(K)} \int_K \lambda_z v \,\mathrm{d}\mathbf{x} = \frac{1}{2\mu_2(K)} \int_K \lambda_z \mathbf{r}_{K,\gamma} \cdot \nabla v \,\mathrm{d}\mathbf{x}.$$

Set $v = |w|^2$, and

$$\begin{aligned}
\frac{1}{\mu_1(\gamma)} \int_\gamma \lambda_z |w|^2 \,\mathrm{d}s - \frac{3}{2\mu_2(K)} \int_K \lambda_z |w|^2 \,\mathrm{d}\mathbf{x} &\leq \frac{1}{2\mu_2(K)} \int_K |\lambda_z \mathbf{r}_{K,\gamma} \cdot \nabla(|w|^2)| \,\mathrm{d}\mathbf{x} \\
&\leq \frac{2h_K}{2\mu_2(K)} \int_K \lambda_z |\nabla w||w| \,\mathrm{d}\mathbf{x} \\
&\leq \frac{2h_K}{2\mu_2(K)} \left\|\lambda_z^{1/2} w\right\|_{\mathrm{L}^2(K)} \left\|\lambda_z^{1/2}\nabla w\right\|_{\mathrm{L}^2(K)}.
\end{aligned}$$

□

In addition, on time intervals I_m, $m = 1, \dots, s$, we introduce an interpolation operator $\Pi^m_{\tau q} : V \to P_q(I_m)$ where V is some function space and $P_q(I_m)$ is a polynomial space of degree q, which is defined by

$$v \in V : \Pi^m_{\tau q} v(t_k) = v(t_k) \qquad k = 0, \dots, q, \tag{14}$$

where $t_k \in I_m$, $k = 0, \dots, q$ are distinct time points. The operator $\Pi^m_{\tau q}$ can be explicitly represented by using the Lagrange basis functions $\mathcal{L}_k$ as

$$\Pi^m_{\tau q} w = \sum_{k=0}^{q} w(t_k) \mathcal{L}_k. \tag{15}$$

Lemma 3.5. *Let $r \in [1, \infty]$, $q \geq 0$ be the polynomial degree, $s \in [0, 1]$ and let t be an integer such that $s \leq t \leq q + 1$. Then, for $w \in \mathrm{W}^{t,r}(I_m)$, the operator $\Pi^m_{\tau q}$ satisfies*

$$\left| w - \Pi^m_{\tau q} w \right|_{\mathrm{W}^{s,r}(I_m)} \leq C \tau_m^{t-s} |w|_{\mathrm{W}^{t,r}(I_m)}, \tag{16}$$

with positive constant C.

Proof. This result follows from a simple Taylor series expansion; cf. Theorem 1.5 of [2]. □

3.2. Reliability

We first derive *a posteriori* upper bounds for the dual norm (9).

Theorem 3.6. *Let $u^\tau_h \in S^{\tau,q}_{h,p}$ be the numerical solution obtained from (5) and $\mathcal{R}$ be the residual defined by (11); then, the following error bound of the dual norm (9) holds*

$$\left\| \mathcal{R}(u^\tau_h) \right\|^2_m \leq \sum_{K \in \mathcal{T}^m_h} \eta_1^2 + \sum_{\gamma \in \mathcal{F}^m_{h,I}} \eta_2^2 + \sum_{\gamma \in \mathcal{F}^m_h} \eta_3^2 + \sum_{K \in \mathcal{T}^m_h} \eta_4^2 \tag{17}$$

for $m = 1, \dots, s$, where

$$\begin{aligned}
\eta_1^2 &= \int_{I_m} \max_{\mathbf{z} \in \mathcal{N}_K} \left(\frac{C_F^2 h_z^2}{h_K^2} \right) h_K^2 \| f + \nabla \cdot \mathbf{K}(u^\tau_h) \nabla u^\tau_h - \partial_t \vartheta(u^\tau_h) \|^2_{\mathrm{L}^2(K)} \, \mathrm{d}t, \\
\eta_2^2 &= \int_{I_m} \max_{\mathbf{z} \in \mathcal{N}_\gamma} \left(\frac{A^2 h_z^2}{h_\gamma} \right) h_\gamma \| \mathbf{n}_\gamma \cdot [\![\mathbf{K}(u^\tau_h) \nabla u^\tau_h]\!] \|^2_{\mathrm{L}^2(\gamma)} \, \mathrm{d}t, \\
\eta_3^2 &= \int_{I_m} \max_{\mathbf{z} \in \mathcal{N}_\gamma} \left(\frac{2A^2 h_z^2}{h_\gamma} \right) h_\gamma \epsilon^2 \| [\![u^\tau_h]\!] \|^2_{\mathrm{L}^2(\gamma)} \, \mathrm{d}t, \\
\eta_4^2 &= (C + 1 + 0.5 C_I)^2 C_F^2 \max_{\mathbf{z} \in \mathcal{N}_K} \left(\frac{h_z^2}{h_K^2} \right) h_K^2 \left\| \lfloor \vartheta(u^\tau_h) \rfloor_{m-1} \right\|^2_{\mathrm{L}^2(K)},
\end{aligned}$$

with $A^2 = \left(3C_F^2 + 2C_F\right) \mu_1(\gamma) \mu_2(K)^{-1} \approx \mathcal{O}(h_K^{-1})$ and $h_z = \max_{K \in \omega_z} h_K$.

Proof. Defining a partition of unity using the nodal hat functions and with a constant function $v_z \in P_0(K)$ we have, by Galerkin orthogonality, that

$$\langle \mathcal{R}(u^\tau_h), v \rangle = \sum_{\mathbf{z} \in \mathcal{N}_h} \langle \mathcal{R}(u^\tau_h), \lambda_z (v - v_z) \rangle_{\omega_z}, \tag{18}$$

where $\langle \cdot, \cdot \rangle_{\omega_z} = \langle \cdot, \cdot \rangle|_{\omega_z}$. We now consider a single vertex $\mathbf{z} \in \mathcal{N}_h$ and let σ_z be the set of edges in the patch ω_z, and define $\sigma_z^I = \sigma_z \cap \mathcal{F}_h^I$. By integration by parts we have that

$$
\begin{aligned}
\langle \mathcal{R}(u_h^\tau), \lambda_z(v-v_z)\rangle_{\omega_z} &= \ell(\lambda_z(v-v_z)) - A_{h,m}(u_h^\tau, \lambda_z(v-v_z)) \\
&= \int_{I_m} \sum_{K\in\omega_z} (f, \lambda_z(v-v_z))_K \,\mathrm{d}t - \int_{I_m} \sum_{K\in\omega_z} (\mathbf{K}(u_h^\tau)\nabla u_h^\tau, \nabla\lambda_z(v-v_z))_K \,\mathrm{d}t \\
&\quad + \int_{I_m} \sum_{\gamma\in\sigma_z} (\mathbf{n}_\gamma \cdot \{\!\{\mathbf{K}(u_h^\tau)\nabla u_h^\tau\}\!\}, [\![\lambda_z(v-v_z)]\!])_\gamma \,\mathrm{d}t - \int_{I_m} \sum_{\gamma\in\sigma_z} \epsilon([\![u_h^\tau]\!], [\![\lambda_z(v-v_z)]\!])_\gamma \,\mathrm{d}t \\
&\quad - \int_{I_m} \sum_{K\in\omega_z} (\partial_t \vartheta(u_h^\tau), \lambda_z(v-v_z))_K \,\mathrm{d}t - \sum_{K\in\omega_z} \left(\lfloor \vartheta(u_h^\tau)\rfloor_{m-1}, \lambda_z(v-v_z)|_{m-1}^+\right)_K \\
&= \int_{I_m} \sum_{K\in\omega_z} (f + \nabla\cdot(\mathbf{K}(u_h^\tau)\nabla u_h^\tau) - \partial_t\vartheta(u_h^\tau), \lambda_z(v-v_z))_K \,\mathrm{d}t \\
&\quad - \int_{I_m} \sum_{\gamma\in\sigma_z^I} (\mathbf{n}_\gamma \cdot [\![\mathbf{K}(u_h^\tau)\nabla u_h^\tau]\!], \{\!\{\lambda_z(v-v_z)\}\!\})_\gamma \,\mathrm{d}t \\
&\quad - \int_{I_m} \sum_{\gamma\in\sigma_z} \epsilon([\![u_h^\tau]\!], [\![\lambda_z(v-v_z)]\!])_\gamma \,\mathrm{d}t - \sum_{K\in\omega_z} \left(\lfloor \vartheta(u_h^\tau)\rfloor_{m-1}, \lambda_z(v-v_z)|_{m-1}^+\right)_K \\
&:= \xi_1 + \xi_2 + \xi_3 + \xi_4. \qquad (19)
\end{aligned}
$$

To estimate the first term ξ_1, we firstly apply the Cauchy–Schwarz inequality and Lemma 3.2 and obtain

$$
\begin{aligned}
|\xi_1| &\le \int_{I_m} \left(\sum_{K\in\omega_z} \left\| \lambda_z^{1/2}(f + \nabla\cdot\mathbf{K}(u_h^\tau)\nabla u_h^\tau) - \partial_t\vartheta(u_h^\tau)\right\|_{\mathrm{L}^2(K)}^2 \right)^{1/2} \left(\sum_{K\in\omega_z} \left\| \lambda_z^{1/2}(v-v_z)\right\|_{\mathrm{L}^2(K)}^2 \right)^{1/2} \mathrm{d}t \\
&\le \int_{I_m} \left(\sum_{K\in\omega_z} \left\| \lambda_z^{1/2}(f + \nabla\cdot\mathbf{K}(u_h^\tau)\nabla u_h^\tau) - \partial_t\vartheta(u_h^\tau)\right\|_{\mathrm{L}^2(K)}^2 \right)^{1/2} \left(\sum_{K\in\omega_z} C_F^2 h_K^2 \left\| \lambda_z^{1/2}\nabla v\right\|_{\mathrm{L}^2(K)}^2 \right)^{1/2} \mathrm{d}t. \qquad (20)
\end{aligned}
$$

Using Cauchy–Schwarz, Lemmas 3.4 and 3.2, the second term of (19), ξ_2, can be estimated as

$$
\begin{aligned}
|\xi_2| &\le \int_{I_m} \left(\sum_{\gamma\in\sigma_z^I} \left\| \lambda_z^{1/2}(\mathbf{n}_\gamma \cdot [\![\mathbf{K}(u_h^\tau)\nabla u_h^\tau]\!])\right\|_{\mathrm{L}^2(\gamma)}^2 \right)^{1/2} \left(\sum_{\gamma\in\sigma_z^I} \left\| \lambda_z^{1/2}\{\!\{v-v_z\}\!\}\right\|_{\mathrm{L}^2(\gamma)}^2 \right)^{1/2} \mathrm{d}t \\
&\le \int_{I_m} \left(\sum_{\gamma\in\sigma_z^I} \left\| \lambda_z^{1/2}(\mathbf{n}_\gamma \cdot [\![\mathbf{K}(u_h^\tau)\nabla u_h^\tau]\!])\right\|_{\mathrm{L}^2(\gamma)}^2 \right)^{1/2} \left(\sum_{K\in\omega_z} A^2 h_K^2 \left\| \lambda_z^{1/2}\nabla v\right\|_{\mathrm{L}^2(K)}^2 \right)^{1/2} \mathrm{d}t. \qquad (21)
\end{aligned}
$$

Similarly, by Cauchy–Schwarz, (13), Lemmas 3.4 and 3.2

$$
\begin{aligned}
|\xi_3| &\le \int_{I_m} \left(\sum_{\gamma\in\sigma_z} \epsilon^2 \left\| \lambda_z^{1/2}[\![u_h^\tau]\!]\right\|_{\mathrm{L}^2(\gamma)}^2 \right)^{1/2} \left(\sum_{\gamma\in\sigma_z} \left\| \lambda_z^{1/2}[\![v-v_z]\!]\right\|_{\mathrm{L}^2(\gamma)}^2 \right)^{1/2} \mathrm{d}t \\
&\le \int_{I_m} \left(\sum_{\gamma\in\sigma_z} \epsilon^2 \left\| \lambda_z^{1/2}[\![u_h^\tau]\!]\right\|_{\mathrm{L}^2(\gamma)}^2 \right)^{1/2} \left(\sum_{K\in\omega_z} 2A^2 h_K^2 \left\| \lambda_z^{1/2}\nabla v\right\|_{\mathrm{L}^2(K)}^2 \right)^{1/2} \mathrm{d}t. \qquad (22)
\end{aligned}
$$

Again by Cauchy–Schwarz we obtain that

$$
\begin{aligned}
|\xi_4| &\le \sum_{K\in\omega_z} \int_K \left|\lambda_z^{1/2}\lfloor\vartheta(u_h^\tau)\rfloor_{m-1}\right| \left|\lambda_z^{1/2}(v-v_z)|_{m-1}^+\right| \mathrm{d}\mathbf{x} \\
&= \sum_{K\in\omega_z} \int_K \frac{1}{2}\left|\lambda_z^{1/2}\lfloor\vartheta(u_h^\tau)\rfloor_{m-1}\right| \left|\lambda_z^{1/2}(v-v_z)|_{m-1}^+ + \lambda_z^{1/2}(v-v_z)|_m^- + \lambda_z^{1/2}(v-v_z)|_{m-1}^+ - \lambda_z^{1/2}(v-v_z)|_m^-\right| \mathrm{d}\mathbf{x}.
\end{aligned}
$$

Using the fact that the trapezoidal rule is exact for the linear (in time) function $\Pi_{\tau 1}^m(\lambda_z^{1/2}(v-v_z)) \in P_1(I_m)$ we have that

$$\int_{I_m} \Pi_{\tau 1}^m\Big(\lambda_z^{1/2}(v-v_z)\Big)\,\mathrm{d}t = \frac{\tau_m}{2}\Big(\lambda_z^{1/2}(v-v_z)|_{m-1}^{+} + \lambda_z^{1/2}(v-v_z)|_m^{-}\Big).$$

Applying this result and the fundamental theorem of calculus gives

$$\begin{aligned}
|\xi_4| &\le \sum_{K\in\omega_z}\int_K \Big|\lambda_z^{1/2}\lfloor\vartheta(u_h^\tau)\rfloor_{m-1}\Big|\left(\left|\frac{1}{\tau_m}\int_{I_m}\Pi_{\tau 1}^m(\lambda_z^{1/2}(v-v_z))\,\mathrm{d}t - \frac{1}{2}\int_{I_m}\partial_t(\lambda_z^{1/2}(v-v_z))\,\mathrm{d}t\right|\right)\mathrm{d}\mathbf{x}\\
&\le \sum_{K\in\omega_z}\int_K \Big|\lambda_z^{1/2}\lfloor\vartheta(u_h^\tau)\rfloor_{m-1}\Big|\left(\frac{1}{\tau_m}\int_{I_m}\Big|\Pi_{\tau 1}^m(\lambda_z^{1/2}(v-v_z)) - \lambda_z^{1/2}(v-v_z)\Big|\,\mathrm{d}t\right.\\
&\quad\left.+\frac{1}{\tau_m}\int_{I_m}\Big|\lambda_z^{1/2}(v-v_z)\Big|\,\mathrm{d}t + \frac{1}{2}\int_{I_m}\Big|\partial_t\Big(\lambda_z^{1/2}(v-v_z)\Big)\Big|\,\mathrm{d}t\right)\mathrm{d}\mathbf{x}\\
&\le \sum_{K\in\omega_z}\int_K \Big|\lambda_z^{1/2}\lfloor\vartheta(u_h^\tau)\rfloor_{m-1}\Big|\left(\Big\|\Pi_\tau\Big(\lambda_z^{1/2}(v-v_z)\Big) - \lambda_z^{1/2}(v-v_z)\Big\|_{\mathrm{L}^2(I_m)}\right.\\
&\quad\left.+\Big\|\lambda_z^{1/2}(v-v_z)\Big\|_{\mathrm{L}^2(I_m)} + \frac{\tau_m}{2}\Big\|\partial_t\Big(\lambda_z^{1/2}(v-v_z)\Big)\Big\|_{\mathrm{L}^2(I_m)}\right)\mathrm{d}\mathbf{x}.
\end{aligned}$$

Setting $D = C+1+0.5C_I$ and applying Cauchy–Schwarz, Minkowski inequality, Lemma 3.2, and the standard inverse inequality $|w|_{\mathrm{H}^1(I_m)} \le C_I\tau_m^{-1}\|w\|_{\mathrm{L}^2(I_m)}$ ([20], Lem. 2.21) gives that

$$\begin{aligned}
|\xi_4| &\le \left(\sum_{K\in\omega_z}\Big\|\lambda_z^{1/2}\lfloor\vartheta(u_h^\tau)\rfloor_{m-1}\Big\|_{\mathrm{L}^2(K)}^2\right)^{1/2}\left(\sum_{K\in\omega_z}D^2\Big\|\lambda_z^{1/2}(v-v_z)\Big\|_{\mathrm{L}^2(I_m,\mathrm{L}^2(K))}^2\right)^{1/2}\\
&\le \left(\sum_{K\in\omega_z}\Big\|\lambda_z^{1/2}\lfloor\vartheta(u_h^\tau)\rfloor_{m-1}\Big\|_{\mathrm{L}^2(K)}^2\right)^{1/2}\left(\int_{I_m}\sum_{K\in\omega_z}D^2C_F^2h_K^2\Big\|\lambda_z^{1/2}\nabla v\Big\|_{\mathrm{H}^1(K)}^2\,\mathrm{d}t\right)^{1/2}. \qquad (23)
\end{aligned}$$

Letting $h_z = \max_{h\in\omega_z}K$ and combining (19)–(23), we have that

$$\begin{aligned}
\langle\mathcal{R}(u_h^\tau),\lambda_z(v-v_z)\rangle_{\omega_z} &\le \left(\int_{I_m}C_F^2h_z^2\sum_{K\in\omega_z}\Big\|\lambda_z^{1/2}(f+\nabla\cdot\mathbf{K}(u_h^\tau)\nabla u_h^\tau) - \partial_t\vartheta(u_h^\tau)\Big\|_{\mathrm{L}^2(K)}^2\,\mathrm{d}t\right)^{1/2}\|v\|_{\mathrm{L}^2(I_m,H^1_\lambda(\omega_z))}\\
&\quad+\left(\int_{I_m}A^2h_z^2\sum_{\gamma^I\in\sigma_z}\Big\|\lambda_z^{1/2}(\mathbf{n}_\gamma\cdot[\![\mathbf{K}(u_h^\tau)\nabla u_h^\tau]\!])\Big\|_{\mathrm{L}^2(\gamma)}^2\,\mathrm{d}t\right)^{1/2}\|v\|_{\mathrm{L}^2(I_m,H^1_\lambda(\omega_z))}\\
&\quad+\left(\int_{I_m}2A^2h_z^2\sum_{\gamma^{ID}\in\sigma_z}\epsilon^2\Big\|\lambda_z^{1/2}[\![u_h^\tau]\!]\Big\|_{\mathrm{L}^2(\gamma)}^2\,\mathrm{d}t\right)^{1/2}\|v\|_{\mathrm{L}^2(I_m,H^1_\lambda(\omega_z))}\\
&\quad+\left(D^2C_F^2h_z^2\sum_{K\in\omega_z}\Big\|\lambda_z^{1/2}\lfloor\vartheta(u_h^\tau)\rfloor_{m-1}\Big\|_{\mathrm{L}^2(K)}^2\right)^{1/2}\|v\|_{\mathrm{L}^2(I_m,H^1_\lambda(\omega_z))},
\end{aligned}$$

where

$$\|v\|_{\mathrm{L}^2(I_m,H^1_\lambda(\omega_z))} := \left(\int_{I_m}\sum_{K\in\omega_z}\Big\|\lambda_z^{1/2}\nabla v\Big\|_{\mathrm{L}^2(K)}^2\,\mathrm{d}t\right)^{1/2}.$$

Then, by (18) and the definition of the dual norm (9), summation over all $\mathbf{z} \in \mathcal{N}_h$ gives

$$\begin{aligned}
\|\!|\mathcal{R}(u_h^\tau)|\!\|_*^2 \le & \sum_{\mathbf{z}\in\mathcal{N}_h} \int_{I_m} C_F^2 h_z^2 \sum_{K\in\omega_z} \left\| \lambda_z^{1/2}(f + \nabla\cdot\mathbf{K}(u_h^\tau)\nabla u_h^\tau) - \partial_t \vartheta(u_h^\tau) \right\|_{\mathrm{L}^2(K)}^2 \mathrm{d}t \\
& + \sum_{\mathbf{z}\in\mathcal{N}_h} \int_{I_m} A^2 h_z^2 \sum_{\gamma^I\in\sigma_z} \left\| \lambda_z^{1/2}(\mathbf{n}_\gamma \cdot [\![\mathbf{K}(u_h^\tau)\nabla u_h^\tau]\!]) \right\|_{\mathrm{L}^2(\gamma)}^2 \mathrm{d}t \\
& + \sum_{\mathbf{z}\in\mathcal{N}_h} \int_{I_m} 2A^2 h_z^2 \sum_{\gamma^{ID}\in\sigma_z} \epsilon^2 \left\| \lambda_z^{1/2} [\![u_h^\tau]\!] \right\|_{\mathrm{L}^2(\gamma)}^2 \mathrm{d}t \\
& + \sum_{\mathbf{z}\in\mathcal{N}_h} D^2 C_F^2 h_z^2 \sum_{K\in\omega_z} \left\| \lambda_z^{1/2} \lfloor \vartheta(u_h^\tau) \rfloor_{m-1} \right\|_{\mathrm{L}^2(K)}^2 .
\end{aligned}$$

We note that

$$\begin{aligned}
& \sum_{\mathbf{z}\in\mathcal{N}_h} \int_{I_m} C_F^2 h_z^2 \sum_{K\in\omega_z} \left\| \lambda_z^{1/2}(f + \nabla\cdot\mathbf{K}(u_h^\tau)\nabla u_h^\tau) - \partial_t \vartheta(u_h^\tau) \right\|_{\mathrm{L}^2(K)}^2 \mathrm{d}t \\
& \quad = \sum_{K\in\mathcal{T}_h^m} \sum_{\mathbf{z}\in\mathcal{N}_K} \int_{I_m} C_F^2 h_z^2 \left\| \lambda_z^{1/2}(f + \nabla\cdot\mathbf{K}(u_h^\tau)\nabla u_h^\tau - \partial_t \vartheta(u_h^\tau)) \right\|_{\mathrm{L}^2(K)}^2 \mathrm{d}t \\
& \quad \le \sum_{K\in\mathcal{T}_h^m} \max_{\mathbf{z}\in\mathcal{N}_K} \left(\frac{C_F^2 h_z^2}{h_K^2} \right) h_K^2 \sum_{\mathbf{z}\in\mathcal{N}_K} \int_{I_m} \left\| \lambda_z^{1/2}(f + \nabla\cdot\mathbf{K}(u_h^\tau)\nabla u_h^\tau - \partial_t \vartheta(u_h^\tau)) \right\|_{\mathrm{L}^2(K)}^2 \mathrm{d}t \\
& \quad = \sum_{K\in\mathcal{T}_h^m} \max_{\mathbf{z}\in\mathcal{N}_K} \left(\frac{C_F^2 h_z^2}{h_K^2} \right) h_K^2 \int_{I_m} \| f + \nabla\cdot\mathbf{K}(u_h^\tau)\nabla u_h^\tau - \partial_t \vartheta(u_h^\tau) \|_{\mathrm{L}^2(K)}^2 \mathrm{d}t = \sum_{K\in\mathcal{T}_h^m} \eta_1^2 .
\end{aligned}$$

Similar calculations for the remaining three terms completes the proof. □

Remark 3.7. In the case of an inhomogeneous boundary condition $u = g$ on $\partial\Omega$ the sum of the η_3 terms becomes

$$\sum_{\gamma\in\mathcal{F}_{h,I}^m} \eta_3^2 + \sum_{\gamma\in\mathcal{F}_{h,D}^m} \eta_{3,D}^2$$

where

$$\eta_{3,D}^2 = \int_{I_m} \max_{\mathbf{z}\in\mathcal{N}_\gamma} \left(\frac{2A^2 h_z^2}{h_\gamma} \right) h_\gamma \epsilon^2 \| u_h^\tau - g \|_{\mathrm{L}^2(\gamma)}^2 \mathrm{d}t.$$

Remark 3.8. We note that compared to other *a posteriori* error analysis of space-time methods, cf. [29], the time jump term η_4^2 does not appear to depend on the time step size τ_m which potentially makes this error bound sub-optimal in time. However, we note that some of the analysis for space-time methods in fact have a dependency on the inverse of the time step size $\mathcal{O}(\tau_m^{-1})$ resulting from the jump term, although these have performed a reconstruction to extend to an integral over the time interval (t_{m-1}, t_m); cf. [22, 23].

3.3. Efficiency

To derive the *a posteriori* lower bounds, we first define bubble functions $\psi_K(x)$ on K and $\psi_\gamma(x)$ on γ, which cut off the neighboring elements and edges; cf. Section 2.3.2 of [48]. To this end, for $m = 1, \ldots, s$ we define ω_γ, $\gamma \in \mathcal{F}_h^m$, as the union of the elements in $\mathcal{T}_h^m$ which share the common edge γ.

Lemma 3.9. *Assume that the functions R and J are piecewise polynomials on $\mathcal{T}_h^m$ up to degree p. Then, for all $K \in \mathcal{T}_h^m$, there exists a function $\psi_K \in \mathrm{H}^1(\Omega)$ with $\operatorname{supp}\psi_K \subset K$ such that*

$$\| \psi_K \|_{\mathrm{L}^2(K)} \le 1, \tag{24}$$

$$\|R\|_{\mathrm{L}^2(K)} \leq \widehat{C}_{I,1}(K) \int_K R\psi_K, \tag{25}$$

$$\|\nabla\psi_K\|_{\mathrm{L}^2(K)} \leq \widehat{C}_{I,2}(K) h_K^{-1} \tag{26}$$

where $\widehat{C}_{I,1}$ *and* $\widehat{C}_{I,2}$ *are positive constants dependent on* p *and* K*. Additionally, for all* $\gamma \in \mathcal{F}_h^m$ *there exists a function* $\psi_\gamma \in \mathrm{H}^1(\Omega)$ *with* $\operatorname{supp}\psi_\gamma \subset \omega_\gamma$ *such that*

$$\|\psi_\gamma\|_{\mathrm{L}^2(\gamma)} \leq 1, \tag{27}$$

$$\|J\|_{\mathrm{L}^2(\gamma)} \leq \widehat{C}_{I,3}(\gamma) \int_\gamma J\psi_\gamma, \tag{28}$$

$$\|\psi_\gamma\|_{\mathrm{L}^2(\omega_\gamma)} \leq \max_{K\in\omega_\gamma} \widehat{C}_{I,4}(\gamma,K) h_\gamma^{1/2} \tag{29}$$

$$\|\nabla\psi_\gamma\|_{\mathrm{L}^2(\omega_\gamma)} \leq \max_{K\in\omega_\gamma} \widehat{C}_{I,5}(\gamma,K) h_\gamma^{-1/2} \tag{30}$$

where $\widehat{C}_{I,3}$*,* $\widehat{C}_{I,4} \geq 1$*, and* $\widehat{C}_{I,5} \geq 1$ *are positive constants dependent on* K*,* γ*, and* p*.*

Proof. The results follow from Theorem 3.58 of [48]. □

Lemma 3.10. *Assume that the functions* R *and* J *are piecewise polynomials on* $\mathcal{T}_h^m \times I_m$ *up to degree* p *in space and degree* q *in time. Then, for all* $K \in \mathcal{T}_h^m$*, there exists a function* $\varphi_K \in \mathrm{L}^2(I_m, \mathrm{H}^1(\Omega))$ *with* $\operatorname{supp}\varphi_K \subset K \times I_m$ *such that*

$$\|\varphi_K\|_{\mathrm{L}^2(I_m,\mathrm{L}^2(K))} \leq C_{I,0}(K, I_m), \tag{31}$$

$$\|R\|_{\mathrm{L}^2(I_m,\mathrm{L}^2(K))} \leq C_{I,1}(K, I_m) \int_{I_m}\int_K R\varphi_K, \tag{32}$$

$$\|\nabla\varphi_K\|_{\mathrm{L}^2(I_m,\mathrm{L}^2(K))} \leq C_{I,2}(K, I_m) h_K^{-1} \tag{33}$$

$$\varphi_K|_{m-1}^{+} = 0 \tag{34}$$

where $C_{I,0}$*,* $C_{I,1}$ *and* $C_{I,2}$ *are positive constants dependent on* p*,* q*,* K*, and* I_m*. Additionally, for all* $\gamma \in \mathcal{F}_h^m$ *there exists a function* $\varphi_\gamma \in \mathrm{L}^2(I_m, \mathrm{H}^1(\Omega))$ *with* $\operatorname{supp}\varphi_\gamma \subset \omega_\gamma \times I_m$ *such that*

$$\|\varphi_\gamma\|_{\mathrm{L}^2(I_m,\mathrm{L}^2(\gamma))} \leq C_{I,6}(\gamma, I_m), \tag{35}$$

$$\|J\|_{\mathrm{L}^2(I_m,\mathrm{L}^2(\gamma))} \leq C_{I,3}(\gamma, I_m) \int_{I_m}\int_\gamma J\varphi_\gamma, \tag{36}$$

$$\|\varphi_\gamma\|_{\mathrm{L}^2(I_m,\mathrm{L}^2(\omega_\gamma))} \leq \max_{K\in\omega_\gamma} C_{I,4}(\gamma, K, I_m) h_\gamma^{1/2} \tag{37}$$

$$\|\nabla\varphi_\gamma\|_{\mathrm{L}^2(I_m,\mathrm{L}^2(\omega_\gamma))} \leq \max_{K\in\omega_\gamma} C_{I,5}(\gamma, K, I_m) h_\gamma^{-1/2} \tag{38}$$

where $C_{I,3}$*,* $C_{I,4} \geq 1$*,* $C_{I,5} \geq 1$ *and* $C_{I,6}$ *are positive constants dependent on* I_m*,* K*,* γ*,* p *and* q*.*

Proof. The polynomial $R(\mathbf{x}, t)$ can be written as

$$R = \sum_{i=0}^{q} R_i(\mathbf{x})\phi_i(t)$$

where R_i is a polynomial of degree p is space, and ϕ_i, $i = 0, \ldots, q$ form a basis of the polynomial space $P_q(I_m)$ which, for simplicity, we assume is an orthogonal basis under integration over I_m; *i.e.*, $\int_{I_m} \phi_i\phi_j \,\mathrm{d}t = 0$ if $i \neq j$.

For a polynomial in I_m, there exists a function χ_m which satisfies identical conditions to (24) and (25), with K replaced by I_m and potentially different constants such that $\chi_m(t_{m-1}) = 0$ and $\chi_m(t_m) = 1$; cf. Theorem 3.58 of [48]. Additionally, for R_i there exists a function satisfying Lemma 3.9. Setting φ_K to a suitable product of these functions we have from (25) and the fact ϕ_i, $i = 1, \dots, q$, form an orthogonal basis that

$$\begin{aligned}
\widehat{C}_{I,1}(K)\widehat{C}_{I,1}(I_m) \int_{I_m}\int_K R\varphi_K\chi_m \,\mathrm{d}\mathbf{x} &\geq \widehat{C}_{I,1}(I_m) \int_{I_m} \sum_{i=1}^n \|R_i(\mathbf{x})\|_{\mathrm{L}^2(K)}\phi_i(t)\chi_m \,\mathrm{d}t \\
&\geq \left(\int_{I_m} \left(\sum_{i=1}^n \|R_i(\mathbf{x})\|_{\mathrm{L}^2(K)}\phi_i(t) \right)^2 \mathrm{d}t \right)^{1/2} \\
&= \left(\int_{I_m} \sum_{i=1}^n \|R_i(\mathbf{x})\|^2_{\mathrm{L}^2(K)}|\phi_i(t)|^2 \,\mathrm{d}t \right)^{1/2} \\
&= \left(\int_{I_m}\int_K \sum_{i=1}^n |R_i(\mathbf{x})|^2|\phi_i(t)|^2 \,\mathrm{d}\mathbf{x}\,\mathrm{d}t \right)^{1/2} \\
&= \left(\int_{I_m}\int_K \left| \sum_{i=1}^n R_i(\mathbf{x})\phi_i(t) \right|^2 \mathrm{d}\mathbf{x}\,\mathrm{d}t \right)^{1/2}
\end{aligned}$$

which proves (32). Equations (31) and (33) are proven trivially *via* Cauchy–Schwarz. The proof of (35)–(38) follows analogously. □

We note that in order to derive the lower bounds for the dual norm of the residual R we use the above inverse inequalities which require polynomial functions. However, in general, the residual R is not a polynomial. Therefore, we note that for $m = 1, \dots, s$

$$\left\langle \overline{\mathcal{R}(u_h^\tau)}, w \right\rangle = \left\langle \overline{\mathcal{R}(u_h^\tau)} - \mathcal{R}(u_h^\tau), w \right\rangle + \langle \mathcal{R}(u_h^\tau), w \rangle,$$

for $w \in \mathrm{L}^2(I_m, \mathrm{H}^1(\Omega, \mathcal{T}_h^m))$, where for a function g we denote by $\overline{g}$ the projection onto $P_q(I_m, S_{h,p}^m)$. We can estimate $\langle \overline{\mathcal{R}(u_h^\tau)} - \mathcal{R}(u_h^\tau), w \rangle$ and $\langle \mathcal{R}(u_h^\tau), w \rangle$ in a similar way to the estimation of the upper bounds. We can now state the lower bounds for the dual norm (9).

Theorem 3.11. *Let $u_h^\tau \in S_{h,p}^{\tau,q}$ be the numerical solution obtained from (5), $\overline{\mathcal{R}(u_h^\tau)}$ be the projection of the residual defined by (11) onto $P_q(I_m, S_{h,p}^m)$; then, the lower bound of the dual norm (9)*

$$\left|\!\left|\!\left| \overline{\mathcal{R}(u_h^\tau)} \right|\!\right|\!\right|_m^2 \geq C \left(\sum_{K \in \mathcal{T}_h^m} \widetilde{\eta}_1^2 + \sum_{\gamma \in \mathcal{F}_h^m} \widetilde{\eta}_2^2 \right)$$

holds for $m = 1, \dots, s$, where

$$\begin{aligned}
\widetilde{\eta}_1^2 &= \int_{I_m} h_K^2 \|f + \nabla \cdot \mathbf{K}(u_h^\tau)\nabla u_h^\tau - \partial_t \vartheta(u_h^\tau)\|^2_{\mathrm{L}^2(K)} \,\mathrm{d}t, \\
\widetilde{\eta}_2^2 &= \int_{I_m} h_\gamma \|\mathbf{n}_\gamma \cdot [\![\mathbf{K}(u_h^\tau)\nabla u_h^\tau]\!]\|^2_{\mathrm{L}^2(\gamma)} \,\mathrm{d}t,
\end{aligned}$$

and C is a positive constant.

Proof. We start by studying $\langle\overline{\mathcal{R}(u_h^\tau)}, v\rangle$, for a specific function $v \in \mathrm{L}^2(I_m, \mathrm{H}^1(\Omega, \mathcal{T}_h^m))$. To this end, we define

$$\begin{aligned}
\alpha_K &= h_K^2 \left\| \overline{f + \nabla\cdot\mathbf{K}(u_h^\tau)\nabla u_h^\tau - \partial_t \vartheta(u_h^\tau)} \right\|_{\mathrm{L}^2(I_m,\mathrm{L}^2(K))} \\
\beta_\gamma &= h_\gamma \left\| \mathbf{n}_\gamma \cdot \left[\!\!\left[\overline{\mathbf{K}(u_h^\tau)\nabla u_h^\tau} \right]\!\!\right] \right\|_{\mathrm{L}^2(I_m,\mathrm{L}^2(\gamma))} \\
\eta_\gamma &= h_\gamma \epsilon \| [\![u_h^\tau]\!] \|_{\mathrm{L}^2(I_m,\mathrm{L}^2(\gamma))} \\
\delta_K &= h_K^2 \left\| \left\lfloor \overline{\vartheta(u_h^\tau)} \right\rfloor_{m-1} \right\|_{\mathrm{L}^2(K)}.
\end{aligned}$$

Using the functions φ_K and φ_γ from Lemma 3.10 we define

$$v_1 = \sum_{K\in\mathcal{T}_h^m} \alpha_K \varphi_K, \qquad v_2 = \sum_{\gamma\in\mathcal{F}_{h,I}^m} \beta_\gamma \varphi_\gamma, \qquad v_3 = \sum_{\gamma\in\mathcal{F}_h^m} \eta_\gamma \varphi_\gamma, \qquad v_4 = \sum_{K\in\mathcal{T}_h^m} \delta_K \varphi_K,$$

and let

$$v = \theta_1 v_1 + \theta_2 v_2 + \theta_3 v_3 + \theta_4 v_4, \tag{39}$$

where $\theta_i \geq 0$, $i = 1, 2, 3, 4$ will be determined later. Then, we have that

$$\left\langle \overline{R(u_h^\tau)}, v \right\rangle = \xi_1 + \xi_2 + \xi_3 + \xi_4, \tag{40}$$

where

$$\begin{aligned}
\xi_1 = \theta_1 &\int_{I_m} \sum_{K\in\mathcal{T}_h^m} \alpha_K \left(\overline{f + \nabla\cdot\mathbf{K}(u_h^\tau)\nabla u_h^\tau - \partial_t\vartheta(u_h^\tau)}, \varphi_K \right)_K \mathrm{d}t \\
&+ \theta_2 \int_{I_m} \sum_{\gamma\in\mathcal{F}_{h,I}^m} \beta_\gamma \left(\overline{f + \nabla\cdot\mathbf{K}(u_h^\tau)\nabla u_h^\tau - \partial_t\vartheta(u_h^\tau)}, \varphi_\gamma \right)_{\omega_\gamma} \mathrm{d}t \\
&+ \theta_3 \int_{I_m} \sum_{\gamma\in\mathcal{F}_h^m} \eta_\gamma \left(\overline{f + \nabla\cdot\mathbf{K}(u_h^\tau)\nabla u_h^\tau - \partial_t\vartheta(u_h^\tau)}, \varphi_\gamma \right)_{\omega_\gamma} \mathrm{d}t \\
&+ \theta_4 \int_{I_m} \sum_{K\in\mathcal{T}_h^m} \delta_K \left(\overline{f + \nabla\cdot\mathbf{K}(u_h^\tau)\nabla u_h^\tau - \partial_t\vartheta(u_h^\tau)}, \varphi_K \right)_K \mathrm{d}t
\end{aligned} \tag{41}$$

$$\xi_2 = -\theta_2 \int_{I_m} \sum_{\gamma\in\mathcal{F}_{h,I}^m} \beta_\gamma \left(\mathbf{n}_\gamma \cdot \left[\!\!\left[\overline{\mathbf{K}(u_h^\tau)\nabla u_h^\tau} \right]\!\!\right], \{\!\{\varphi_\gamma\}\!\} \right)_\gamma \mathrm{d}t - \theta_3 \int_{I_m} \sum_{\gamma\in\mathcal{F}_h^m} \eta_\gamma \left(\mathbf{n}_\gamma \cdot \left[\!\!\left[\overline{\mathbf{K}(u_h^\tau)\nabla u_h^\tau} \right]\!\!\right], \{\!\{\varphi_\gamma\}\!\} \right)_\gamma \mathrm{d}t \tag{42}$$

$$\xi_3 = -\theta_2 \int_{I_m} \sum_{\gamma\in\mathcal{F}_{h,I}^m} \beta_\gamma \epsilon ([\![u_h^\tau]\!], [\![\varphi_\gamma]\!])_\gamma \,\mathrm{d}t - \theta_3 \int_{I_m} \sum_{\gamma\in\mathcal{F}_h^m} \eta_\gamma \epsilon ([\![u_h^\tau]\!], [\![\varphi_\gamma]\!])_\gamma \,\mathrm{d}t \tag{43}$$

$$\begin{aligned}
\xi_4 = -\theta_1 &\sum_{K\in\mathcal{T}_h^m} \alpha_K \left(\left\lfloor \overline{\vartheta(u_h^\tau)} \right\rfloor_{m-1}, \varphi_K|_{m-1}^+ \right)_K - \theta_2 \sum_{\gamma\in\mathcal{F}_{h,I}^m} \beta_\gamma \left(\left\lfloor \overline{\vartheta(u_h^\tau)} \right\rfloor_{m-1}, \varphi_\gamma|_{m-1}^+ \right)_{\omega_\gamma} \\
&- \theta_3 \sum_{\gamma\in\mathcal{F}_h^m} \eta_\gamma \left(\left\lfloor \overline{\vartheta(u_h^\tau)} \right\rfloor_{m-1}, \varphi_\gamma|_{m-1}^+ \right)_{\omega_\gamma} - \theta_4 \sum_{K\in\mathcal{T}_h^m} \delta_K \left(\left\lfloor \overline{\vartheta(u_h^\tau)} \right\rfloor_{m-1}, \varphi_K|_{m-1}^+ \right)_K.
\end{aligned} \tag{44}$$

We note that $\varphi_K|_{m-1}^+ = 0$, $\{\!\{\varphi_\gamma\}\!\} = \varphi_\gamma$ and $[\![\varphi_\gamma]\!] = 0$; hence, $\xi_3 = 0$ and $\xi_4 = 0$.

We first estimate the four terms of (41) individually. For the first term, using (32), we have the lower bound

$$\sum_{K\in\mathcal{T}_h^m}\int_{I_m}\alpha_K\Big(\overline{f+\nabla\cdot\mathbf{K}(u_h^\tau)\nabla u_h^\tau-\partial_t\vartheta(u_h^\tau)},\varphi_K\Big)_K\,\mathrm{d}t$$
$$\geq\left(\max_{K\in\mathcal{T}_h^m}C_{I,1}(K,I_m)\right)^{-1}\sum_{K\in\mathcal{T}_h^m}h_K^2\left\|\overline{f+\nabla\cdot\mathbf{K}(u_h^\tau)\nabla u_h^\tau-\partial_t\vartheta(u_h^\tau)}\right\|^2_{\mathrm{L}^2(I_m,\mathrm{L}^2(K))}.$$

By applying the Cauchy–Schwarz inequality, (37), the definition of β_γ and the fact that $h_\gamma\leq h_K$ we bound the second term of ξ_1 as

$$\sum_{\gamma\in\mathcal{F}_{h,I}^m}\int_{I_m}\beta_\gamma\Big(\overline{f+\nabla\cdot\mathbf{K}(u_h^\tau)\nabla u_h^\tau-\partial_t\vartheta(u_h^\tau)},\varphi_\gamma\Big)_{\omega_\gamma}\,\mathrm{d}t$$
$$\leq\sum_{\gamma\in\mathcal{F}_{h,I}^m}\max_{K\in\omega_\gamma}C_{I,4}(\gamma,K,I_m)\sum_{K\in\omega_\gamma}\beta_\gamma h_\gamma^{1/2}\int_{I_m}\left\|\overline{f+\nabla\cdot\mathbf{K}(u_h^\tau)\nabla u_h^\tau-\partial_t\vartheta(u_h^\tau)}\right\|_{\mathrm{L}^2(K)}\mathrm{d}t$$
$$\leq\max_{K\in\mathcal{T}_h^m,\gamma\in\partial K}C_{I,4}(\gamma,K,I_m)\left(\sum_{\gamma\in\mathcal{F}_{h,I}^m}h_\gamma\left\|\mathbf{n}_\gamma\cdot\left[\!\left[\overline{\mathbf{K}(u_h^\tau)\nabla u_h^\tau}\right]\!\right]\right\|^2_{\mathrm{L}^2(I_m,\mathrm{L}^2(\gamma))}\right)^{1/2}$$
$$\times\left(\sum_{K\in\mathcal{T}_h^m}h_K^2\left\|\overline{f+\nabla\cdot\mathbf{K}(u_h^\tau)\nabla u_h^\tau-\partial_t\vartheta(u_h^\tau)}\right\|^2_{\mathrm{L}^2(I_m,\mathrm{L}^2(K))}\right)^{1/2}.$$

Analogously for the third term of ξ_1 we have that

$$\sum_{\gamma\in\mathcal{F}_h^m}\int_{I_m}\eta_\gamma\Big(\overline{f+\nabla\cdot\mathbf{K}(u_h^\tau)\nabla u_h^\tau-\partial_t\vartheta(u_h^\tau)},\varphi_\gamma\Big)_{\omega_\gamma}\,\mathrm{d}t$$
$$\leq\max_{K\in\mathcal{T}_h^m,\gamma\in\partial K}C_{I,4}(\gamma,K,I_m)\left(\sum_{K\in\mathcal{T}_h^m}h_\gamma\epsilon^2\|[\![u_h^\tau]\!]\|^2_{\mathrm{L}^2(I_m,\mathrm{L}^2(K))}\right)^{1/2}$$
$$\times\left(\sum_{K\in\mathcal{T}_h^m}h_K^2\left\|\overline{f+\nabla\cdot\mathbf{K}(u_h^\tau)\nabla u_h^\tau-\partial_t\vartheta(u_h^\tau)}\right\|^2_{\mathrm{L}^2(I_m,\mathrm{L}^2(K))}\right)^{1/2}.$$

Similarly, by the Cauchy–Schwarz inequality and (31), the last term of ξ_1 is bounded as

$$\sum_{K\in\mathcal{T}_h^m}\int_{I_m}\delta_K\Big(\overline{f+\nabla\cdot\mathbf{K}(u_h^\tau)\nabla u_h^\tau-\partial_t\vartheta(u_h^\tau)},\varphi_K\Big)_K\,\mathrm{d}t$$
$$\leq\max_{K\in\mathcal{T}_h^m}C_{I,0}(K,I_m)\sum_{K\in\mathcal{T}_h^m}\delta_K\left\|\overline{f+\nabla\cdot\mathbf{K}(u_h^\tau)\nabla u_h^\tau-\partial_t\vartheta(u_h^\tau)}\right\|_{\mathrm{L}^2(I_m,\mathrm{L}^2(K))}$$
$$\leq\max_{K\in\mathcal{T}_h^m}C_{I,0}(K,I_m)\left(\sum_{K\in\mathcal{T}_h^m}h_K^2\left\|\left\lfloor\overline{\vartheta(u_h^\tau)}\right\rfloor_{m-1}\right\|^2_{\mathrm{L}^2(K)}\right)^{1/2}$$
$$\times\left(\sum_{K\in\mathcal{T}_h^m}h_K^2\left\|\overline{f+\nabla\cdot\mathbf{K}(u_h^\tau)\nabla u_h^\tau-\partial_t\vartheta(u_h^\tau)}\right\|^2_{\mathrm{L}^2(I_m,\mathrm{L}^2(K))}\right)^{1/2}.$$

Now, we estimate the two terms of ξ_2 (42). By (36), we obtain a lower bound for the first term of ξ_2 as

$$-\sum_{\gamma\in\mathcal{F}_{h,I}^m}\int_{I_m}\beta_\gamma\Big(\mathbf{n}_\gamma\cdot\Big[\!\Big[\overline{\mathbf{K}(u_h^\tau)\nabla u_h^\tau}\Big]\!\Big],\varphi_\gamma\Big)_\gamma\,\mathrm{d}t\geq\left(\max_{\gamma\in\mathcal{F}_h^m}C_{I,3}(\gamma,I_m)\right)^{-1}\sum_{\gamma\in\mathcal{F}_{h,I}^m}h_\gamma\Big\|\mathbf{n}_\gamma\cdot\Big[\!\Big[\overline{\mathbf{K}(u_h^\tau)\nabla u_h^\tau}\Big]\!\Big]\Big\|^2_{\mathrm{L}^2(I_m,\mathrm{L}^2(\gamma))}.$$

By employing Cauchy–Schwarz and (35), the second term of ξ_2 can be estimated as

$$\begin{aligned}
&-\sum_{\gamma\in\mathcal{F}_h^m}\int_{I_m}\eta_\gamma\Big(\mathbf{n}_\gamma\cdot\overline{[\![\mathbf{K}(u_h^\tau)\nabla u_h^\tau]\!]},\varphi_\gamma\Big)_\gamma\,\mathrm{d}t\\
&\quad\leq\max_{\gamma\in\mathcal{F}_h^m}C_{I,6}(\gamma,I_m)\sum_{\gamma\in\mathcal{F}_h^m}h_\gamma\epsilon\|[\![u_h^\tau]\!]\|_{\mathrm{L}^2(I_m,\mathrm{L}^2(\gamma))}\Big\|\mathbf{n}_\gamma\cdot\Big[\!\Big[\overline{\mathbf{K}(u_h^\tau)\nabla u_h^\tau}\Big]\!\Big]\Big\|_{\mathrm{L}^2(I_m,\mathrm{L}^2(\gamma))}\\
&\quad\leq\max_{\gamma\in\mathcal{F}_h^m}C_{I,6}(\gamma,I_m)\left(\sum_{\gamma\in\mathcal{F}_h^m}h_\gamma\epsilon^2\|[\![u_h^\tau]\!]\|^2_{\mathrm{L}^2(I_m,\mathrm{L}^2(\gamma))}\right)^{1/2}\left(\sum_{\gamma\in\mathcal{F}_h^m}h_\gamma\Big\|\mathbf{n}_\gamma\cdot\Big[\!\Big[\overline{\mathbf{K}(u_h^\tau)\nabla u_h^\tau}\Big]\!\Big]\Big\|^2_{\mathrm{L}^2(I_m,\mathrm{L}^2(\gamma))}\right)^{1/2}.
\end{aligned}$$

Combining all these results into (40), applying Young's inequality, and setting $C_1=\max_{K\in\mathcal{T}_h^m}C_{I,1}$, $C_2=\max_{K\in\mathcal{T}_h^m}C_{I,0}$, $C_3=\max_{\gamma\in\mathcal{F}_h^m}C_{I,3}$, $C_4=\max_{K\in\mathcal{T}_h^m,\gamma\in\partial K}C_{I,4}$, and $C_5=\max_{K\in\mathcal{T}_h^m,\gamma\in\partial K}C_{I,6}$ gives

$$\begin{aligned}
\langle\overline{R},v\rangle&\geq\left(\theta_1C_1^{-1}-\frac{1}{2}\theta_2C_3C_4^2-\frac{1}{2}\theta_3C_4-\frac{1}{2}\theta_4C_2\right)\sum_{K\in\mathcal{T}_h^m}h_K^2\Big\|\overline{f+\nabla\cdot\mathbf{K}(u_h^\tau)\nabla u_h^\tau-\partial_t\vartheta(u_h^\tau)}\Big\|^2_{\mathrm{L}^2(I_m,\mathrm{L}^2(K))}\\
&\quad+\left(\theta_2C_3^{-1}-\frac{1}{2}\theta_2C_3^{-1}-\frac{1}{2}\theta_3C_6\right)\sum_{\gamma\in\mathcal{F}_h^m}h_\gamma\Big\|\mathbf{n}_\gamma\cdot\Big[\!\Big[\overline{\mathbf{K}(u_h^\tau)\nabla u_h^\tau}\Big]\!\Big]\Big\|^2_{\mathrm{L}^2(I_m,\mathrm{L}^2(\gamma))}\\
&\quad-\frac{1}{2}\theta_3(C_4+C_6)\sum_{\gamma\in\mathcal{F}_h^m}h_\gamma\epsilon^2\|[\![u_h^\tau]\!]\|^2_{\mathrm{L}^2(I_m,\mathrm{L}^2(\gamma))}\\
&\quad-\frac{1}{2}\theta_4C_2\sum_{K\in\mathcal{T}_h^m}h_K^2\Big\|\Big\lfloor\overline{\vartheta(u_h^\tau)}\Big\rfloor_{m-1}\Big\|^2_{\mathrm{L}^2(K)}.
\end{aligned}$$

As all four terms must be non-negative, we must set $\theta_3=\theta_4=0$; then, we select θ_1 and θ_2 such that

$$\theta_1C_1^{-1}-\theta_2C_3C_4^2\geq0,$$

which gives that

$$\langle\overline{R},v\rangle\geq\widehat{C}\left(\sum_{K\in\mathcal{T}_h^m}\widetilde{\eta}_1^2+\sum_{\gamma\in\mathcal{F}_h^m}\widetilde{\eta}_2^2\right)\tag{45}$$

where $\widehat{C}$ is a positive constant. Now, applying (31), (33), (37) and (38) we have, noting that $\theta_3=\theta_4=0$, that

$$\begin{aligned}
\|v\|_{\mathrm{L}^2(I_m,\mathrm{H}^1(\Omega,\mathcal{T}_h^m))}&\leq\theta_1\sum_{K\in\mathcal{T}_h^m}\alpha_K\|\varphi_K\|_{\mathrm{L}^2(I_m,\mathrm{H}^1(K))}+\theta_2\sum_{\gamma\in\mathcal{F}_h^m}\beta_\gamma\|\varphi_\gamma\|_{\mathrm{L}^2(I_m,\mathrm{H}^1(\omega_\gamma,\mathcal{T}_h^m))}\\
&\leq\theta_1\sum_{K\in\mathcal{T}_h^m}\widetilde{C}_1h_K^{-1}\alpha_K+\theta_2\sum_{\gamma\in\mathcal{F}_h^m}\max_{K\in\omega_\gamma}\widetilde{C}_2h_\gamma^{-1/2}\beta_\gamma\\
&=\theta_1\sum_{K\in\mathcal{T}_h^m}\widetilde{C}_1h_K\Big\|\overline{f+\nabla\cdot\mathbf{K}(u_h^\tau)\nabla u_h^\tau-\partial_t\vartheta(u_h^\tau)}\Big\|_{\mathrm{L}^2(I_m,\mathrm{L}^2(K))}\\
&\quad+\theta_2\sum_{\gamma\in\mathcal{F}_h^m}\max_{K\in\omega_\gamma}\widetilde{C}_2h_\gamma^{1/2}\Big\|\mathbf{n}_\gamma\cdot\Big[\!\Big[\overline{\mathbf{K}(u_h^\tau)\nabla u_h^\tau}\Big]\!\Big]\Big\|_{\mathrm{L}^2(I_m,\mathrm{L}^2(\gamma))},
\end{aligned}$$

where $\widetilde{C}_1 = \max(C_{I,0}(K, I_m)C_h, C_{I,2}(K, I_m))$ and $\widetilde{C}_2 = \max(C_{I,4}(K, I_m)C_h, C_{I,5}(K, I_m))$ given a constant $C_h \leq \operatorname{diam}(\Omega)$ such that $h_K \leq C_h$ for all $K \in \mathcal{T}_h^m$. Hence,

$$\|v\|_{\mathrm{L}^2(I_m,\mathrm{H}^1(\Omega,\mathcal{T}_h^m))} \leq \widetilde{C}\left(\sum_{K\in\mathcal{T}_h^m} \widetilde{\eta}_1^2 + \sum_{\gamma\in\mathcal{F}_h^m} \widetilde{\eta}_2^2\right)^{1/2}, \tag{46}$$

where $\widetilde{C}$ is a positive constant. Combining (45) and (46) we have that

$$\left\|\left\|\overline{\mathcal{R}(u_h^\tau)}\right\|\right\|_m = \sup_{w\in\mathrm{L}^2(I_m,\mathrm{H}^1(\Omega,\mathcal{T}_h^m))\setminus\{0\}} \frac{\left\langle \overline{\mathcal{R}(u_h^\tau)}, w\right\rangle}{\|w\|_{\mathrm{L}^2(I_m,\mathrm{H}^1(\Omega,\mathcal{T}_h^m))}} \geq \frac{\left\langle \overline{\mathcal{R}(u_h^\tau)}, v\right\rangle}{\|v\|_{\mathrm{L}^2(I_m,\mathrm{H}^1(\Omega,\mathcal{T}_h^m))}} \geq C\left(\sum_{K\in\mathcal{T}_h^m} \widetilde{\eta}_1^2 + \sum_{\gamma\in\mathcal{F}_h^m} \widetilde{\eta}_2^2\right)^{1/2}$$

where C is a positive constant. □

Remark 3.12. We note that we do not have lower bounds in terms of η_3 and η_4.

4. Numerical experiments

In this section, we perform two numerical experiments to test the performance of the *a posteriori* error bound in Theorem 3.6 within an automated adaptive refinement routine with fixed time step size. We note that it would be advisable to use an adaptive time step size; see, for example, [21, 23]. At each time step we solve the system of nonlinear equations using a simple fixed point iteration with initial guess given by the previous time step (or projection of the initial condition); for each inner iteration we solve the system of linear equations using the Multifrontal Massively Parallel Solver (MUMPS); cf. [4–6].

The mesh $\mathcal{T}_h^m$, at each time step $m = 1, \ldots, s$ is constructed by performing h-adaptive mesh refinement based on marking 20% of elements with the largest elemental error indicators, which are the restriction of the error bound from Theorem 3.6 to each element, for refinement and the 5% with the smallest error indicators for coarsening. This is repeated at each time step until the error bound reaches a desired tolerance 4×10^{-3}. The initial mesh $\mathcal{T}_h^m$ at step $m = 2, \ldots, s$ is constructed by performing h-refinement of the previous mesh $\mathcal{T}_h^{m-1}$ with the smallest 50% marked for coarsening and the largest 1% marked for refinement.

We note that we cannot compute the dual norm of the residual; however, we can compare the convergence of the error bound to the $\mathrm{L}^2(I_m, \mathrm{H}^1(\Omega, \mathcal{T}_h^m))$- and $\mathrm{L}^2(I_m, \mathrm{L}^2(\Omega, \mathcal{T}_h^m))$-error.

4.1. Barenblatt problem

For the first example, by setting $\vartheta(u) = \theta(u) = u^{1/n}$ and $\mathbf{K} = \mathbf{I}$ we consider the Barenblatt problem

$$\partial_t u^{1/n} - \Delta u = 0 \qquad \text{in } (-6, 6)^2 \times (0, 2)$$

for $n > 0$ with the analytical solution

$$u(\mathbf{x}, t) = \frac{1}{t+1}\left[1 - \frac{n-1}{4n^2}\frac{|\mathbf{x}^2|}{(t+1)^{1/n}}\right]_+^{n/n-1},$$

where $[a]_+ = \max(a, 0)$. We first consider $n = 0.2$, which is *fast-diffusion* problem and set suitable initial and boundary conditions. We consider the space-time discretization with space polynomial degree $p = 2$ and time polynomial degree $q = 1$ with fixed time step size $\tau_m = 0.02$, $m = 1, \ldots, 100$.

In Figure 1a we plot the error bound from Theorem 3.6 at each time step and each iteration of the adaptive refinement, along with the actual error in the $\mathrm{L}^2(I_m, \mathrm{H}^1(\Omega, \mathcal{T}_h^m))$- and $\mathrm{L}^2(I_m, \mathrm{L}^2(\Omega, \mathcal{T}_h^m))$-norms. We note that even though the error bound is not for the $\mathrm{L}^2(I_m, \mathrm{H}^1(\Omega, \mathcal{T}_h^m))$-error, it appears to overestimate this error by a

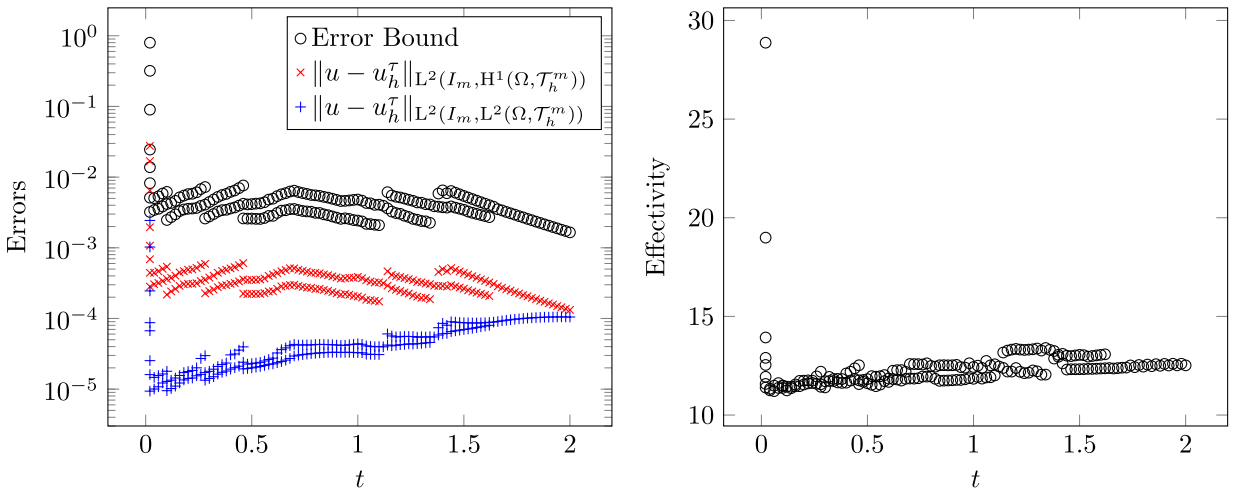

(A) Errors (B) Effectivity

FIGURE 1. Barenblatt problem ($n = 0.2$). Error bound, actual error, and effectivity at each time step and mesh refinement step.

roughly constant amount, which can be seen in Figure 1b where we compute an effectivity index by dividing the error bound by the $\mathrm{L}^2(I_m, \mathrm{H}^1(\Omega, \mathcal{T}_h^m))$-error.

In Figure 2 we show the final mesh at time step $m = 1, 10, 50$ alongside the numerical solution u_h^τ. We note that at $m = 1$ refinement produced by the error indicators is concentrated around the peak at the origin, and as the solution diffuses (at $m = 10, 50$) the mesh coarsens around this origin, while keeping similar refinement in the rest of the domain.

We also consider the Barenblatt problem for $n = 2, 4$, which is the more traditional porous media case. In this situation, in order for the resulting linear systems to be solveable we instead solve the formulation for a $v = u^{1/n}$; namely, we derive a numerical approximation v_h^τ to the equation

$$\partial_t v - \nabla \cdot (n|v|^{n-1}\nabla v) = 0 \qquad \text{in } (-6, 6)^2 \times (0, 2)$$

and then compute $u_h^\tau = (v_h^\tau)^n$. We note that for $n = 4$ we increase the desired tolerance to 0.1 as continuing the refinement further would produce very refined, and difficult to read, meshes; cf. Figure 5.

In Figures 3a and 3b we plot the error bound from Theorem 3.6 at each time step and each iteration of the adaptive refinement for $m = 2, 4$, respectively, along with the actual error in the $\mathrm{L}^2(I_m, \mathrm{H}^1(\Omega, \mathcal{T}_h^m))$- and $\mathrm{L}^2(I_m, \mathrm{L}^2(\Omega, \mathcal{T}_h^m))$-norms. Again, we note that even though the error bound is not for the $\mathrm{L}^2(I_m, \mathrm{H}^1(\Omega, \mathcal{T}_h^m))$-error, it appears to overestimate this error by a roughly constant amount. However, the effectivity index in Figure 3c indicates that this overestimation is not completely constant. We remark here, that especially at coarse mesh resolutions the actual error norms may be incorrect as they are calculated using numerical integration elementwise, and on an insufficiently refined mesh the analytical solution may be badly approximated by the quadrature. Notably, on the first mesh, changing the number of quadrature points ± 1 results in large changes in the computed error; however, this effect disappears on more refined meshes.

Figures 4 and 5 show the final mesh at time step $m = 1, 10, 50$ alongside the numerical solution u_h^τ for $m = 2, 4$, respectively. We note here that a sharp discontinuity in the gradient occurs around the base of the "hill", which we note is captured by the refinement at $m = 1$ produced by the error indicators and which moves outwards from the origin as time evolves (at $m = 10, 50$) with some minor coarsening caused by the discontinuity becoming less sharp. Additionally, as time evolves the mesh around the peak at the origin is coarsened as the

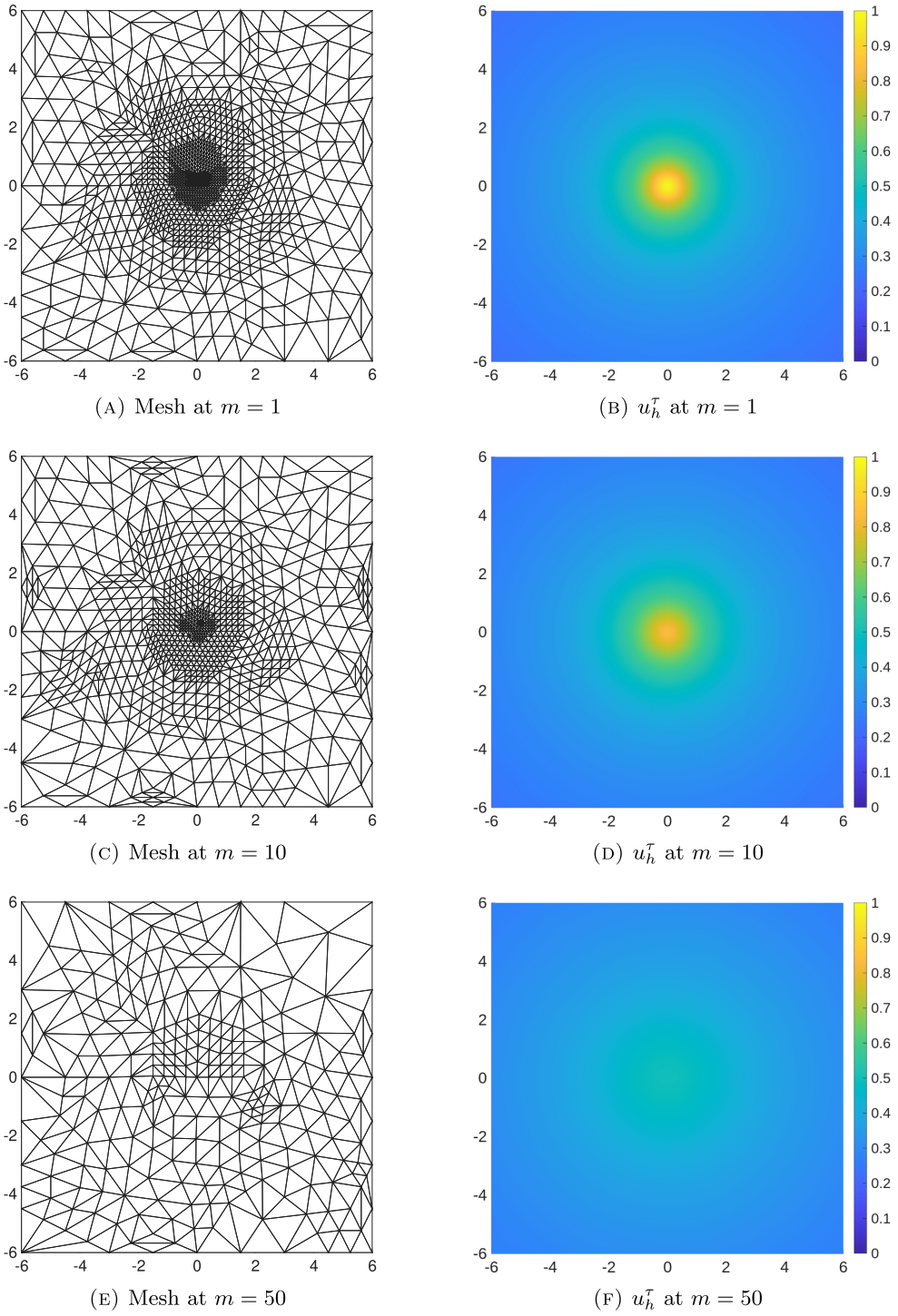

(A) Mesh at $m = 1$ (B) u_h^τ at $m = 1$

(C) Mesh at $m = 10$ (D) u_h^τ at $m = 10$

(E) Mesh at $m = 50$ (F) u_h^τ at $m = 50$

FIGURE 2. Barenblatt problem ($n = 0.2$). Final meshes compared to solution at $m = 1, 10, 50$.

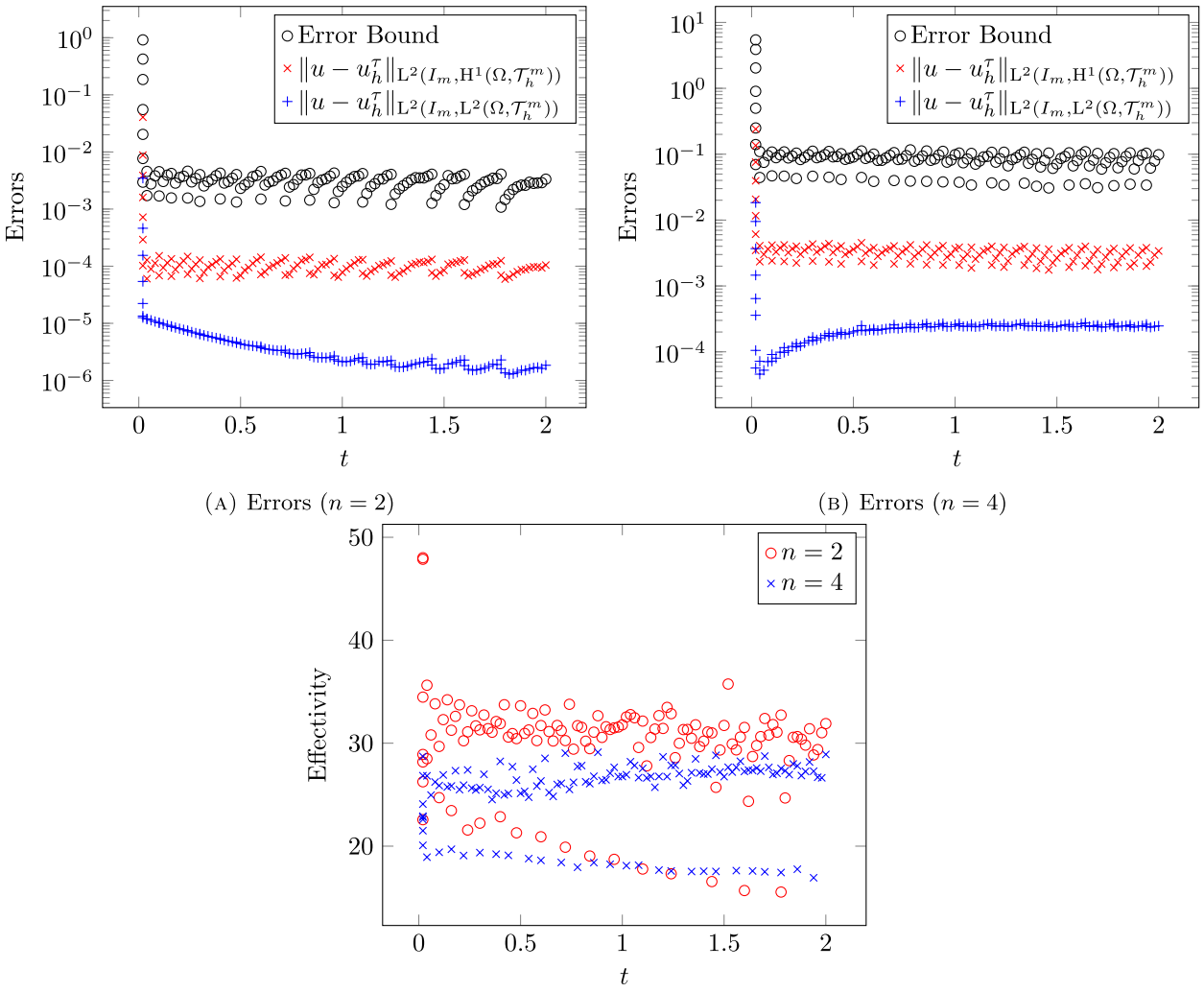

(A) Errors ($n = 2$)

(B) Errors ($n = 4$)

(C) Effectivity

FIGURE 3. Barenblatt problem ($n = 2, 4$). Error bound, actual error, and effectivity at each time step and mesh refinement step.

peak diffuses. We note that the layer is sharper in the $m = 4$ case resulting in more refinement around this layer.

4.2. Tracy problem

For this problem we consider the equation (1) on $\Omega = (0, 1) \times (0, 2)$ with $f = 0$ and $T = 0.001$ with the Gardner [33] constitutive relationships. We set

$$\theta(u) = \begin{cases} \theta_S & \text{if } u \geq 0, \\ \theta_R + (\theta_S - \theta_R)e^{Au} & \text{if } u < 0, \end{cases}$$

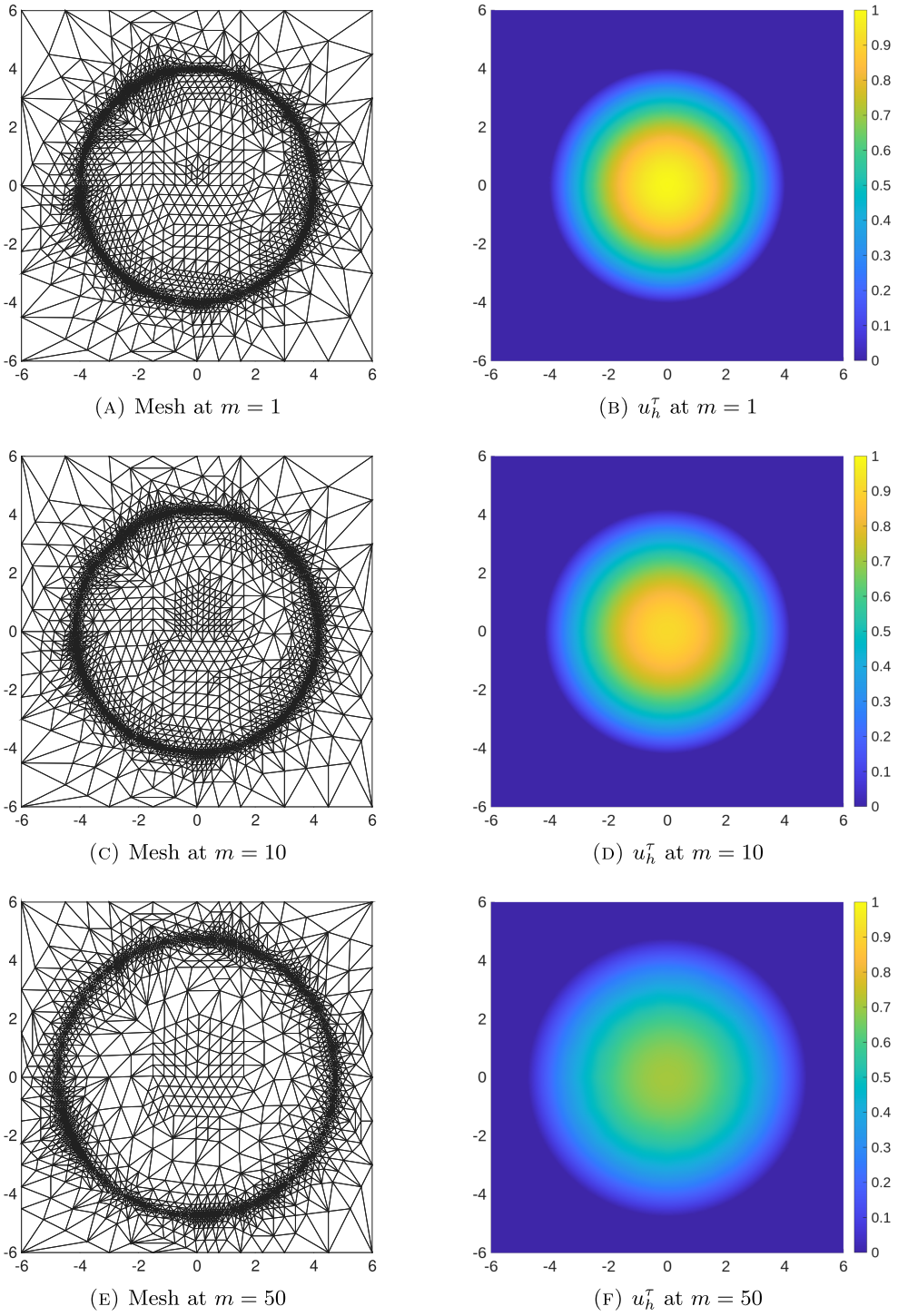

(A) Mesh at $m = 1$ (B) u_h^τ at $m = 1$

(C) Mesh at $m = 10$ (D) u_h^τ at $m = 10$

(E) Mesh at $m = 50$ (F) u_h^τ at $m = 50$

FIGURE 4. Barenblatt problem ($n = 2$). Final meshes compared to solution at $m = 1, 10, 50$.

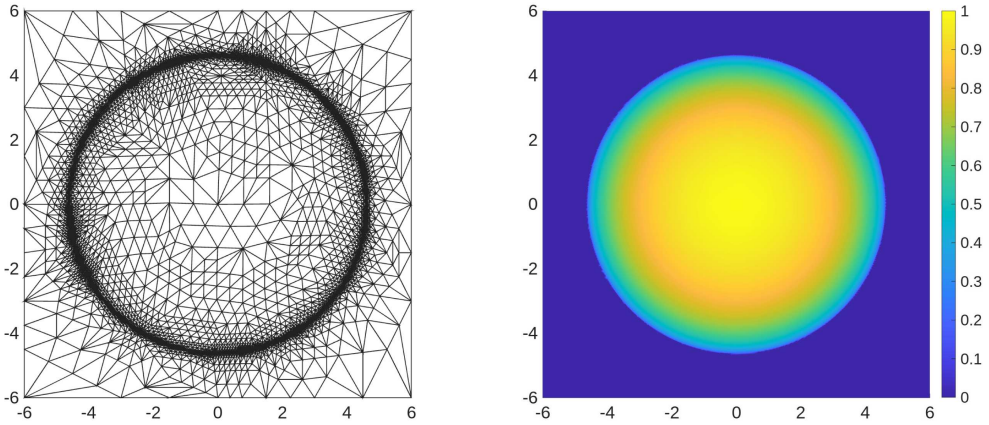

(A) Mesh at $m = 1$

(B) u_h^τ at $m = 1$

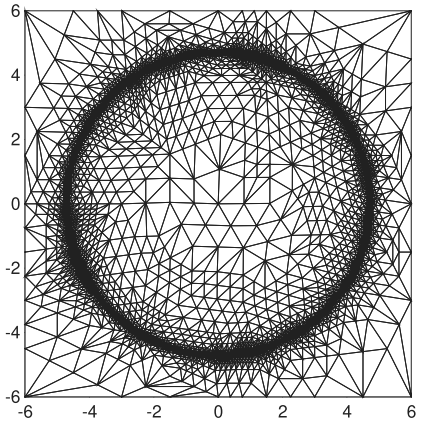

(C) Mesh at $m = 10$

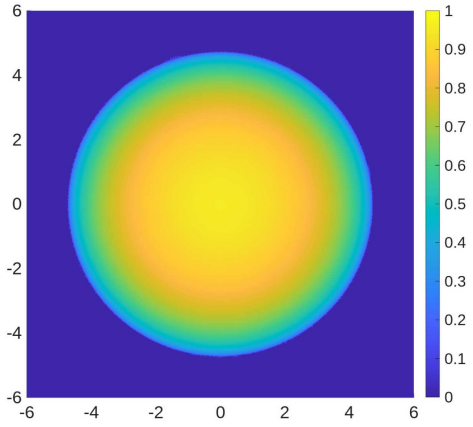

(D) u_h^τ at $m = 10$

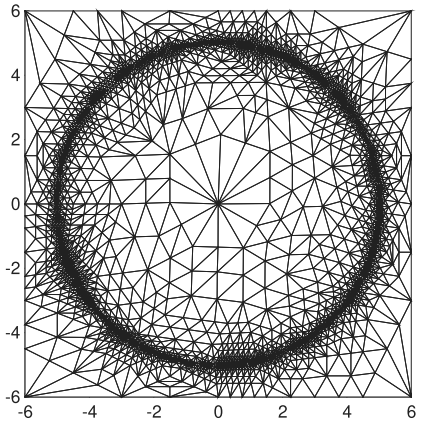

(E) Mesh at $m = 50$

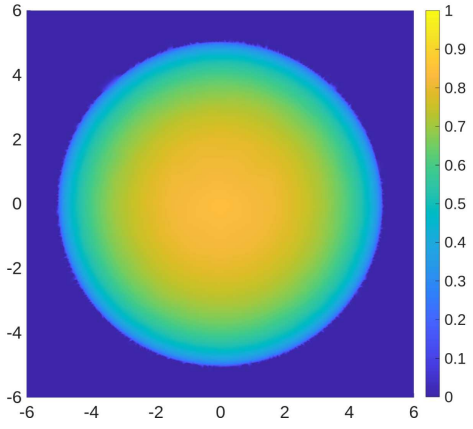

(F) u_h^τ at $m = 50$

FIGURE 5. Barenblatt problem ($n = 4$). Final meshes compared to solution at $m = 1, 10, 50$.

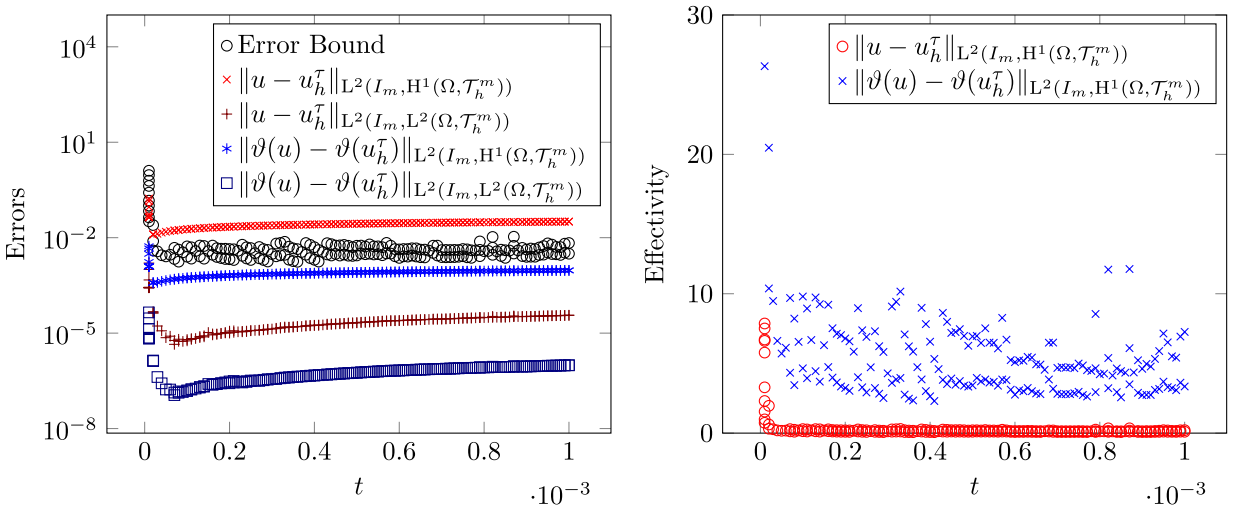

(A) Errors (B) Effectivity

FIGURE 6. Tracy problem. Error bound, actual error, and effectivity at each time step and mesh refinement step.

$$\mathbf{K}(u) = \begin{cases} K_S \mathbf{I} & \text{if } u \geq 0, \\ K_S \mathbf{I} e^{Au} & \text{if } u < 0, \end{cases}$$

with $A = 0.1$, $K_S = 1.1$, $\theta_S = 0.5$, and $\theta_R = 0$. We set the initial condition $u_0 = -10$ on the whole domain Ω, and define inhomogeneous Dirichlet boundary conditions of -10 on every edge, except the $y = 2$ (top) edge, where we set the boundary condition to

$$\log\left(e^{Au_0} + \left(1 - e^{Au_0}\right)\right) \sin(\pi/A).$$

We refer to [45, 46] for the analytical solution.

Remark 4.1. We note that the solution u should not be positive due to the maximum principle; however, we consider $u > 0$ as the STDG formulation considered here does not guarantee the preservation of the maximum principle for the numerical solution. In practice, the solution does appear to stay non-positive; cf. Figure 7.

We note that we have an inconsistency between the initial and boundary conditions. To allow for this, we only solve the first time step to the tolerance 4×10^{-2}. For this problem, we consider the space-time discretization with space polynomial degree $p = 2$ and time polynomial degree $q = 1$ with fixed time step size $\tau_m = 10^{-5}$, $m = 1, \ldots, 100$.

In Figure 6a we plot the error bound from Theorem 3.6 at each time step and each iteration of the adaptive refinement, along with the actual error in the $\mathrm{L}^2(I_m, \mathrm{H}^1(\Omega, \mathcal{T}_h^m))$- and $\mathrm{L}^2(I_m, \mathrm{L}^2(\Omega, \mathcal{T}_h^m))$-norms. Additionally, we also include $\mathrm{L}^2(I_m, \mathrm{H}^1(\Omega, \mathcal{T}_h^m))$- and $\mathrm{L}^2(I_m, \mathrm{L}^2(\Omega, \mathcal{T}_h^m))$-norms for ϑ to show that the error in the active pore volume behaves similarly to the pressure variable. In this problem, we note that the error bound underestimates the $\mathrm{L}^2(I_m, \mathrm{H}^1(\Omega, \mathcal{T}_h^m))$-error. This is confirmed in Figure 1b where we compute an effectivity index by dividing the error bound by the $\mathrm{L}^2(I_m, \mathrm{H}^1(\Omega, \mathcal{T}_h^m))$-error, where this value is below 1. Additionally, we also compute an effectivity index for the $\mathrm{L}^2(I_m, \mathrm{H}^1(\Omega, \mathcal{T}_h^m))$-error of ϑ, which we notice the error indicator overestimates, and with an effectivity which fluctuates.

We again show in Figure 7 the final mesh at time step $m = 1, 5, 25$ compared to the numerical solution. We note that the refinement follows the front of the solution with coarsening as the solution diffuses; notably, at $m = 1$ there is a sharp layer at $y = 2$, but this is more diffused at $m = 25$.

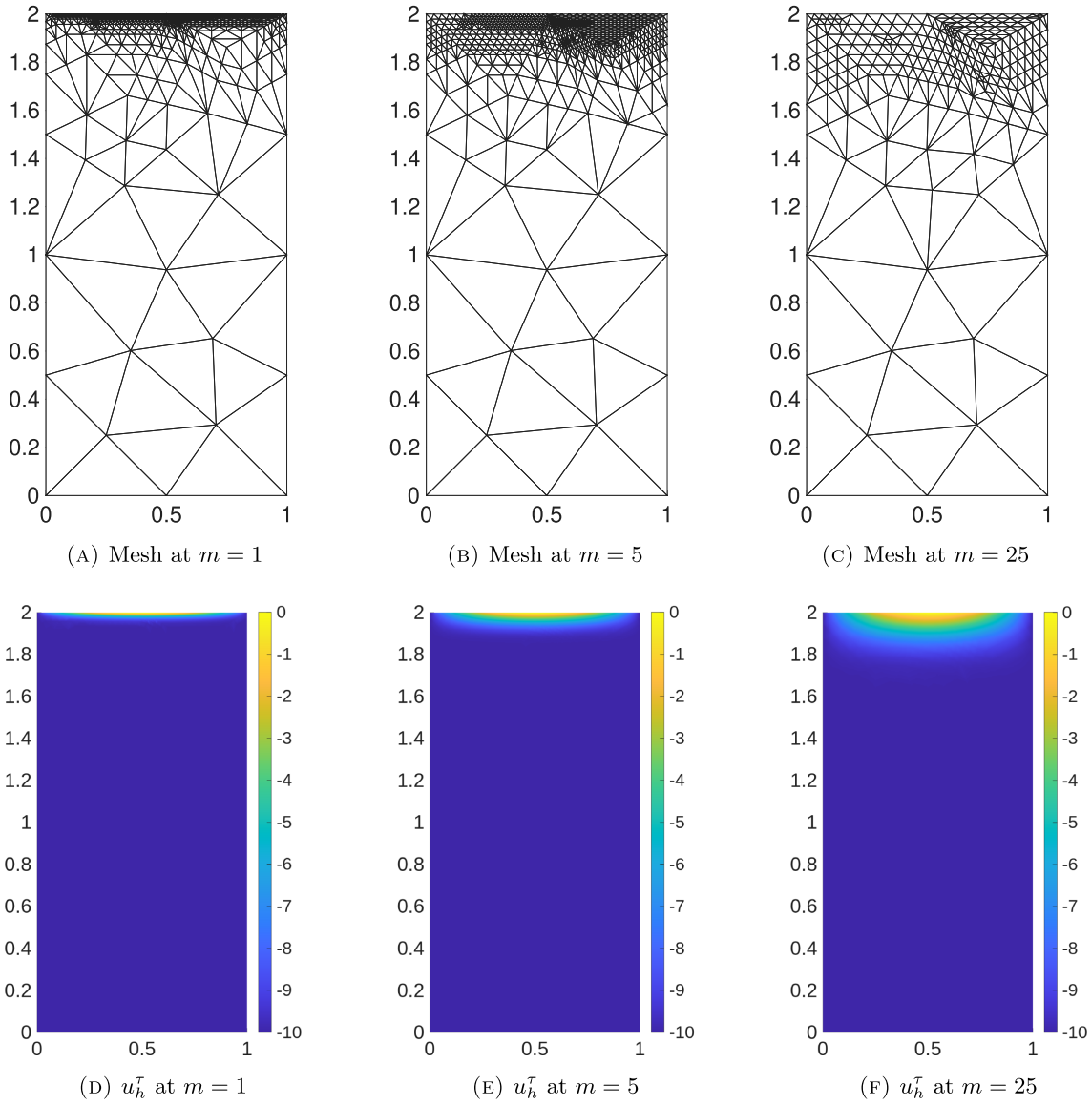

(A) Mesh at $m = 1$ (B) Mesh at $m = 5$ (C) Mesh at $m = 25$

(D) u_h^τ at $m = 1$ (E) u_h^τ at $m = 5$ (F) u_h^τ at $m = 25$

FIGURE 7. Tracy problem. Final meshes compared to solution at $m = 1, 5, 25$.

4.3. Brooks–Corey problem

For the final problem, we consider a more realistic simulation resembling a Brooks–Corey model; cf. Section 6.3 of [38]. For this problem we consider, on the domain $\Omega = (0,1)^2$, a slightly different version of the differential equation,

$$\partial_t S(p) - \nabla \cdot \left(\widehat{\mathbf{K}}(S(p))(\nabla p + \mathbf{g}) \right) = 0 \qquad \text{in } \Omega \times (0,1), \tag{47}$$

where p is the pressure and $S(p)$ is the saturation. We note that we can consider this equation the same as (1) by setting $u = p + \mathbf{g}\cdot\mathbf{x}$, $\vartheta(u) = S(u - \mathbf{g}\cdot\mathbf{x})$, $\mathbf{K}(u) = \widehat{\mathbf{K}}(\vartheta(u))$, and $f = 0$ in (1). Additionally, we set

$$\mathbf{g} = -\mathbf{e}_x, \qquad S(p) = \begin{cases} \frac{1}{(2-p)^{1/3}} & \text{if } p < 1, \\ 1 & \text{if } p \geq 1, \end{cases}, \qquad \widehat{\mathbf{K}}(s) = \overline{\mathbf{K}} s^3,$$

where $\mathbf{e}_x$ is the unit vector in the x-direction and $\overline{\mathbf{K}} \in \mathbb{R}^{2\times 2}$ is a matrix denoting the properties of the medium. In this example, we consider a heterogeneous and anisotropic medium with

$$\overline{\mathbf{K}} = \begin{cases} \overline{\mathbf{K}}_1 & \text{for } x < 0.5, \\ 0.1\mathbf{Q}^\top \overline{\mathbf{K}}_1 \mathbf{Q} & \text{for } x \geq 0.5, \end{cases} \quad \text{where } \overline{\mathbf{K}}_1 = \begin{pmatrix} 1 & 0 \\ 0 & 0.5 \end{pmatrix}, \quad \mathbf{Q} = \begin{pmatrix} \cos \pi/3 & -\sin \pi/3 \\ \sin \pi/3 & \cos \pi/3 \end{pmatrix}.$$

We also consider inhomogeneous Dirichlet conditions $p = p_{\text{in}} = 0.8$ on the boundary $\{0\} \times (0, 0.5)$ and $p = p_{\text{out}} = -3$ on the boundary $(0.5, 1) \times \{1\}$, and homogeneous Neumann boundary conditions on the rest of the boundary. We note that we have not considered the analysis of Neumann boundary conditions in this article; therefore, to perform the simulation we consider the following changes to the formulation and error indicators:

- in the form $a_{h,m}(u, v)$, cf. (7), we change all integrals over edges to be *only* integrals over interior edges and edges on the Dirichlet boundary, and
- the error indicator η_3, cf. (17), is not calculated for edges on the Neumann boundary.

This problem does not have a known analytical solution; therefore, we use the initial condition

$$u_0 = \begin{cases} p_{\text{in}} + \mathbf{g}\cdot\mathbf{x}, & x < 0.5, \\ p_{\text{out}} + \mathbf{g}\cdot\mathbf{x}, & x \geq 0.5 \end{cases}$$

to conform with the boundary. For this problem, we consider the space-time discretization with space polynomial degree $p = 2$ and time polynomial degree $q = 1$ with fixed time step size $\tau_m = 0.01$, $m = 1, \ldots, 100$. We additionally start with a uniform mesh in order to accurately capture the interface between the materials.

As we cannot compare the error bound to the true error, we only display the meshes generated and the numerical solution at several time steps in Figure 8 to demonstrate the performance of the error indicator. We first note that we use a fairly high tolerance, 0.9, due to the high level of refinement that otherwise occurs at the point $(0.5, 1)$. As can be seen in the meshes, the refinement at the initial steps is concentrated around the discontinuity in the initial solution between the two materials, as well as at the points between the Dirichlet and Neumann boundaries at $(0, 0.5)$ and $(0.5, 1)$. As time evolves, the refinement around the point $(0.5, 1)$ becomes more refined along with refinement on the boundary $(0.5, 1) \times \{1\}$, while the rest of the domain is coarsened towards the initial mesh as the discontinuity at the material interface becomes smooth. We also note that as time evolves a portion of the domain around $(0.5, 0)$ becomes fully saturated. We have highlighted the vertices of the mesh where this occurs on the plot of the saturation at each time step.

5. Conclusion

In this article, we have studied the numerical approximation of the Richards equation using a space-time discontinuous Galerkin formulation. We have derived both upper and lower *a posteriori* error bounds for error in a residual dual norm. These error bounds are based on extending residual based arguments from continuous spatial metheds to a discontinuous space-time formulation, and are computable just from the numerical solution without solving an additional formulation or problem. We have provided several numerical approximations where the mesh is adapted at each subinterval of time based on local error indicators from the error estimate. In these numerical experiments we note that while the error bound is not a bound on the actual error in the H^1-norm it does behave similarly to the actual error and the mesh adapts according to how the solution evolves in time. While the error bound is, therefore, not a true bound on the error, it can be used to drive adaptive refinement as it is able to approximate areas in the mesh where the error is likely to be large.

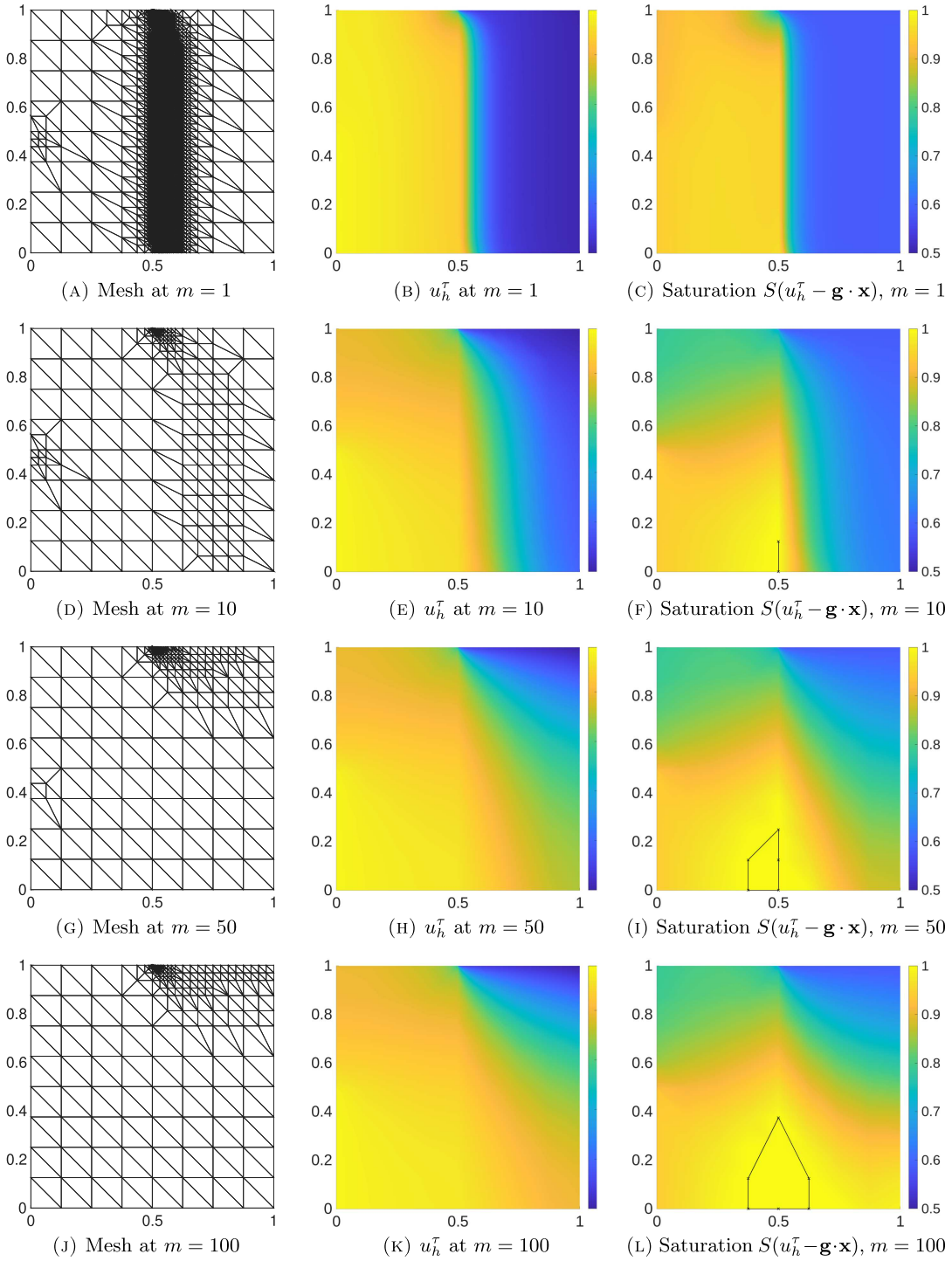

(A) Mesh at $m = 1$ (B) u_h^τ at $m = 1$ (C) Saturation $S(u_h^\tau - \mathbf{g} \cdot \mathbf{x})$, $m = 1$

(D) Mesh at $m = 10$ (E) u_h^τ at $m = 10$ (F) Saturation $S(u_h^\tau - \mathbf{g} \cdot \mathbf{x})$, $m = 10$

(G) Mesh at $m = 50$ (H) u_h^τ at $m = 50$ (I) Saturation $S(u_h^\tau - \mathbf{g} \cdot \mathbf{x})$, $m = 50$

(J) Mesh at $m = 100$ (K) u_h^τ at $m = 100$ (L) Saturation $S(u_h^\tau - \mathbf{g} \cdot \mathbf{x})$, $m = 100$

FIGURE 8. Brooks–Corey problem. Final meshes compared to solutions at $m = 1, 10, 50, 100$. The region where the solution is in the saturated regime is marked on the saturation solution.

Funding

The first author (S.C) was supported by Charles University Research programme number PRIMUS/22/SCI/014.

Data availability statement

The research data associated with this article are included in the article.

References

[1] E. Ahmed, S. Ali Hassan, C. Japhet, M. Kern and M. Vohralík, A posteriori error estimates and stopping criteria for space-time domain decomposition for two-phase flow between different rock types. *SMAI J. Comput. Math.* **5** (2019) 195–227.

[2] M. Ainsworth and J.T. Oden, A Posteriori Error Estimation in Finite Element Analysis. John Wiley & Sons (2000).

[3] H.W. Alt and S. Luckhaus, Quasilinear elliptic-parabolic differential equations. *Math. Z* **183** (1983) 311–341.

[4] P.R. Amestoy, I.S. Duff and J.-Y. L'Excellent, Multifrontal parallel distributed symmetric and unsymmetric solvers. *Comput. Methods Appl. Mech. Eng.* **184** (2000) 501–520.

[5] P.R. Amestoy, I.S. Duff, J. Koster and J.-Y. L'Excellent, A fully asynchronous multifrontal solver using distributed dynamic scheduling. *SIAM J. Matrix Anal. App.* **23** (2001) 15–41.

[6] P.R. Amestoy, A. Guermouche, J.-Y. L'Excellent and S. Pralet, Hybrid scheduling for the parallel solution of linear systems. *Parallel Comput.* **32** (2006) 136–156.

[7] T. Arbogast, M. Wheeler and N.-Y. Zhang, A nonlinear mixed finite element method for a degenerate parabolic equation arising in flow in porous media. *SIAM J. Numer. Anal.* **33** (1996) 1669–1687.

[8] D.N. Arnold, F. Brezzi, B. Cockburn and L.D. Marini, Unified analysis of discontinuous Galerkin methods for elliptic problems. *SIAM J. Numer. Anal.* **39** (2002) 1749–1779.

[9] I. Babuška, M. Feistauer and P. Šolín, On one approach to a posteriori error estimates for evolution problems solved by the method of lines. *Numer. Math.* **89** (2001) 225–256.

[10] V. Baron, Y. Coudière and P. Sochala, Adaptive multistep time discretization and linearization based on a posteriori error estimates for the Richards equation. *Appl. Numer. Math.* **112** (2017) 104–125.

[11] P. Bastian, A fully-coupled discontinuous Galerkin method for two-phase flow in porous media with discontinuous capillary pressure. *Comput. Geosci.* **18** (2014) 779–796.

[12] M. Berardi and F.V. Difonzo, Strong solutions for Richards' equation with Cauchy conditions and constant pressure gradient. *Environ. Fluid Mech.* **20** (2020) 165–174.

[13] C. Bernardi, L. El Alaoui and Z. Mghazli, A posteriori analysis of a space and time discretization of a nonlinear model for the flow in partially saturated porous media. *IMA J. Numer. Anal.* **34** (2014) 1002–1036.

[14] D. Braess, V. Pillwein and J. Schöberl, Equilibrated residual error estimates are p-robust. *Comput. Methods Appl. Mech. Eng.* **198** (2009) 1189–1197.

[15] C. Cancès, F. Nabet and M. Vohralík, Convergence and a posteriori error analysis for energy-stable finite element approximations of degenerate parabolic equations. *Math. Comput.* **90** (2021) 517–563.

[16] J.-B. Clément, F. Golay, M. Ersoy and D. Sous, An adaptive strategy for discontinuous Galerkin simulations of Richards' equation: application to multi-materials dam wetting. *Adv. Water Resour.* **151** (2021) 103897.

[17] S. Congreve, V. Dolejší and S. Sakić, Error analysis for local discontinuous Galerkin semidiscretization of Richards' equation. *IMA J. Numer. Anal.* **45** (2025) 580–630.

[18] E. DiBenedetto, Degenerate Parabolic Equations. Springer, New York (1993).

[19] V. Dolejší, A. Ern and M. Vohralík, A framework for robust a posteriori error control in unsteady nonlinear advection-diffusion problems. *SIAM J. Numer. Anal.* **51** (2013) 773–793.

[20] V. Dolejší and M. Feistauer, Discontinuous Galerkin Method: Analysis and Applications to Compressible Flow. Vol. 48. Springer (2015).

[21] V. Dolejší, M. Kuraz and P. Solin, Adaptive higher-order space-time discontinuous Galerkin method for the computer simulation of variably-saturated porous media flows. *Appl. Math. Modell.* **72** (2019) 276–305.

[22] V. Dolejší, F. Roskovec and M. Vlasák, A posteriori error estimates for higher order space-time Galerkin discretizations of nonlinear parabolic problems. *SIAM J. Numer. Anal.* **59** (2021) 1486–1509.

[23] V. Dolejší, H.-G. Shin and M. Vlasák, Error estimates and adaptivity of the space-time discontinuous Galerkin method for solving the Richards equation. *J. Sci. Comput.* **101** (2024) 1–39.

[24] C. Ebmeyer, Error estimates for a class of degenerate parabolic equations. *SIAM J. Numer. Anal.* **35** (1998) 1095–1112.
[25] L. El Alaoui, An adaptive finite volume box scheme for solving a class of nonlinear parabolic equations. *Appl. Math. Lett.* **22** (2009) 291–296.
[26] Y. Epshteyn and B. Rivière, Analysis of *hp* discontinuous Galerkin methods for incompressible two-phase flow. *J. Comput. Appl. Math.* **225** (2009) 487–509.
[27] K. Eriksson and C. Johnson, Adaptive finite element methods for parabolic problems IV: nonlinear problems. *SIAM J. Numer. Anal.* **32** (1995) 1729–1749.
[28] A. Ern and M. Vohralík, A posteriori error estimation based on potential and flux reconstruction for the heat equation. *SIAM J. Numer. Anal.* **48** (2010) 198–223.
[29] A. Ern, I. Smears and M. Vohralík, Guaranteed, locally space-time efficient, and polynomial-degree robust a posteriori error estimates for high-order discretizations of parabolic problems. *SIAM J. Numer. Anal.* **55** (2017) 2811–2834.
[30] R. Eymard, M. Gutnic and D. Hilhorst, The finite volume method for Richards equation. *Comput. Geosci.* **3** (1999) 259–294.
[31] R. Eymard, D. Hilhorst and M. Vohralík, A combined finite volume-nonconforming/mixed-hybrid finite element scheme for degenerate parabolic problems. *Numer. Math.* **105** (2006) 73–131.
[32] M.W. Farthing and F.L. Ogden, Numerical solution of Richards' equation: a review of advances and challenges. *Soil Sci. Soc. Am. J.* **81** (2017) 1257–1269.
[33] W.R. Gardner, Some steady-state solutions of the unsaturated moisture flow equation with application to evaporation from a water table. *Soil Sci.* **85** (1958) 228–232.
[34] I.C. Kim and N. Požár, Nonlinear elliptic–parabolic problems. *Arch. Ration. Mech. Anal.* **210** (2013) 975–1020.
[35] C. Kreuzer, Reliable and efficient a posteriori error estimates for finite element approximations of the parabolic-Laplacian. *Calcolo* **50** (2013) 79–110.
[36] H. Li, M. Farthing and C. Miller, Adaptive local discontinuous Galerkin approximation to Richards' equation. *Adv. Water Resour.* **30** (2007) 1883–1901.
[37] F. List and F.A. Radu, A study on iterative methods for solving Richards' equation. *Comput. Geosci.* **20** (2016) 341–353.
[38] K. Mitra and M. Vohralík, A posteriori error estimates for the Richards equation. *Math. Comput.* **93** (2024) 1053–1096.
[39] R.H. Nochetto and C. Verdi, Approximation of degenerate parabolic problems using a numerical integration. *SIAM J. Numer. Anal.* **25** (1988) 784–814.
[40] M. Ohlberger, Convergence of a mixed finite elements-finite volume method for the two phase flow in porous media. *East-West J. Numer. Math.* **5** (1997) 183–210.
[41] F. Radu, I. Pop and P. Knabner, Error estimates for a mixed finite element discretization of some degenerate parabolic equations. *Numer. Math.* **109** (2008) 285–311.
[42] L.A. Richards, Capillary conduction of liquids through porous mediums. *J. Appl. Phys.* **1** (1931) 318–333.
[43] S. Sakić, *Numerical solution of degenerate parabolic problems*. Ph.D. thesis, Charles University, Prague, Czech Republic (2024). https://dspace.cuni.cz/handle/20.500.11956/195165.
[44] H.-G. Shin, *A posteriori error estimates and adaptivity for solving the Richards equation*. Ph.D. thesis, Charles University, Prague, Czech Republic (2025). https://dspace.cuni.cz/handle/20.500.11956/198009.
[45] P. Solin and M. Kuraz, Solving the nonstationary Richards equation with adaptive *hp*-FEM. *Adv. Water Resour.* **34** (2011) 1062–1081.
[46] F.T. Tracy, Clean two- and three-dimensional analytical solutions of Richards' equation for testing numerical solvers. *Water Resour. Res.* **42** (2006). DOI: 10.1029/2005WR004638.
[47] T. Tran and T.-B. Duong, A complete analysis for some a posteriori error estimates with the finite element method of lines for a nonlinear parabolic equation. *Numer. Funct. Anal. Optim.* **23** (2002) 891–909.
[48] R. Verfürth, A Posteriori Error Estimation Techniques for Finite Element Methods. Oxford University Press, Oxford, UK (2013).
[49] C.S. Woodward and C.N. Dawson, Analysis of expanded mixed finite element methods for a nonlinear parabolic equation modeling flow into variably saturated porous media. *SIAM J. Numer. Anal.* **37** (2000) 701–724.
[50] I. Yotov, Mixed finite element discretization on non-matching multiblock grids for a degenerate parabolic equation arising in porous media flow. *East-West J. Numer. Math.* **5** (1997) 211–230.